

# Using a novel application for Mixed Reality navigated orthopaedic implant placement: a pilot study

S.R. Stoutjesdijk



This page is intentionally left blank

# Using a novel application for Mixed Reality navigated orthopaedic implant placement: a pilot study

Stephanie Stoutjesdijk

Student number: 4557808

27 September 2023

Thesis in partial fulfilment of the requirements for the joint degree of Master of Science in

## *Technical Medicine*

Leiden University; Delft University of Technology; Erasmus University Rotterdam

Master thesis project (TM30004; 35 ECTS)

Dept. of Orthopaedic Surgery, UMC Utrecht  
3 October 2022 – 27 September 2023

Supervisors:

Prof. dr. ir. Harrie Weinans  
Dr. Bart van der Wal  
Chien Nguyen, MSc

Thesis committee members:

Prof. dr. ir. Harrie Weinans, TU Delft (chair)  
Dr. Bart van der Wal, UMC Utrecht  
Chien Nguyen, MSc, UMC Utrecht  
Dr. Roy van den Ende, LUMC

An electronic version of this thesis is available at <http://repository.tudelft.nl>

# Acknowledgements

This thesis marks the culmination of my journey as an MSc Technical Medicine student. The past 7 years have been a great adventure in which I had the opportunity to learn about a wide range of topics. My main interest has always revolved around innovations in surgical interventions, so I was thrilled to get the opportunity to conduct the final stretch of the journey at the orthopedic department in collaboration with the 3D Lab of UMC Utrecht. I would like to express my gratitude to Harrie, Bart and Chien for their pivotal roles in making this project possible and guiding me along the way.

Beyond from my official supervisors, I also extend my appreciation to Prof. Meij and Drs. Kwananocha from the Veterinary Small Animal Clinic of the Utrecht University for their support and participation in this project. Placing implants on phantoms, a cadaver and even a try-out in an in vivo case would not have been possible without your help. I would also like to thank the HoloMA team in Bulgaria (Stoyan, Nikolay, Atanas) for their technical support and all the meetings dedicated to enhancing the software. Also many thanks to ir. Magré for designing all personalized implants for this project, and a shout-out to Jeroen and Bart from the Technical Department and Joël from the FaceLab for 3D-printing all tools and implants.

I must also acknowledge my fellow graduate students from floor Q2 (Florianne, Laura, Laurens, Marjet, Mijs, Manouk and Suzan). We did many coffee and tea breaks together and the lunch breaks were always very pleasant. It was a pleasure to share ideas about the varying individual projects we were working on. I also have to apologize to you for all distractions in the room whenever I was working with the HoloLens and making silly movements with my hands in the air to interact with the virtual content. But don't worry, these entertainment sessions of 'apple picking' will probably be continued by Roan!

Last but certainly not least, I must thank my dad for his unwavering support. Not only during this thesis project, but throughout my time as a student. You kicked my ass whenever I was feeling down to continue working hard to reach my goals as a student as well as a motocross racer. Thanks to you I was able to combine the university life with participation at the motocross world championship series every single year (at least when I was not injured). Without your support I probably would not be able to say that I am about to obtain my university master's degree! I hope mama will be very proud of me.

Cheers,

Stephanie

# Abstract

## Introduction

Augmented Reality (AR) and Mixed Reality (MR) can be used for surgical navigation to execute the pre-operative plan. HoloMA is a novel AR/MR application which can guide the user to place surgical instruments on the planned location within the patient. In this pilot study, the AR/MR-guidance of HoloMA was used to place personalized canine acetabular roof implants on the pre-planned location on the iliac bone.

## Methods

Dedicated tools to perform the AR/MR patient registration and surgical guidance were developed. An in silico patient registration test was conducted to assess if the available bony surface during the acetabular roof surgery was suitable to perform the patient registration accurately. Pilot tests to place implants using the AR/MR-guidance of HoloMA were conducted on phantoms, a cadaver and in an in vivo dog patient. The translational and angulation error between the planned and the post-operative implant positions were determined. The aim was to achieve implant placement with a maximum translational error of 4.0 mm and a maximum angulation error of 5.0° relative to the pre-operative plan.

## Results

The in silico patient registration test demonstrated a mean translational error of  $0.94 \pm 0.23$  mm and a mean angulation error of  $2.49 \pm 0.34^\circ$ . In the phantom tests, implants (n=6) were placed with a mean translational error of  $1.94 \pm 0.79$  mm. The mean angulation errors in this test were:  $2.87 \pm 1.81^\circ$  (transversal plane),  $1.72 \pm 1.64^\circ$  (dorsal plane) and  $3.10 \pm 2.52^\circ$  (sagittal plane). Two of the implants of the phantom test and both implants of the cadaveric test (n=2) were positioned with a translational error exceeding 4.0 mm and/or angulation error exceeding 5.0° from the planned positions. No implants were placed using AR/MR-guidance in the in vivo dog patient test.

## Conclusion

The results of the in silico patient registration test hold promise for the use of AR/MR-guidance in positioning personalized acetabular roof implants. However, the moderate outcomes observed in the phantom and cadaveric test suggest the need for further testing and improvements before deploying this AR/MR technology in a clinical setting.

## List of contents

Abstract .....	4
1 Introduction.....	6
1.1 Medical background .....	6
1.2 Technical background.....	7
1.3 Research aim .....	9
1.4 Thesis outline.....	9
2 Patient registration.....	10
2.1 Introduction.....	10
2.2 Methods .....	10
2.3 Results .....	13
2.4 Discussion .....	17
3 Surgical navigation .....	19
3.1 Introduction.....	19
3.2 Methods .....	19
3.3 Results .....	20
3.4 Discussion .....	23
4 Implant position accuracy .....	25
4.1 Introduction.....	25
4.2 Methods .....	25
4.3 Results .....	30
4.4 Discussion .....	34
5 General discussion.....	35
6 Conclusion .....	36
7 References.....	37
7 Appendixes .....	39
Appendix A: Implant position on phantoms .....	39
Appendix B: Implant position on cadaver .....	42

# 1 Introduction

## 1.1 Medical background

Hip dysplasia is a medical condition characterized by a shallow and/or vertically oriented hip socket (acetabulum) (Figure 1), which can result in various issues such as pain, hip dislocation, and leg length discrepancy. In infants diagnosed with hip dysplasia, the initial treatment typically involves the use of braces, with or without closed reduction, to reposition the femoral head within the acetabulum. If this initial treatment is not successful or if the condition is diagnosed later, pelvic osteotomies may be recommended to reorient the acetabulum and increase the coverage of the femoral head. (1) If the dysplasia is left untreated, the articular cartilage will be exposed to increased pressure per unit of area due to a smaller contact surface. Osteoarthritis (OA) will develop as a response to the cartilage failure. (2)

One commonly used surgical technique for pelvic osteotomy is the peri-acetabular osteotomy (PAO), which has been in use since the 1970s. The PAO involves rotating the acetabulum to improve its alignment (Figure 2). However, this procedure is associated with a long rehabilitation period with and high complication rates, ranging between 6% and 37%. (3,4)

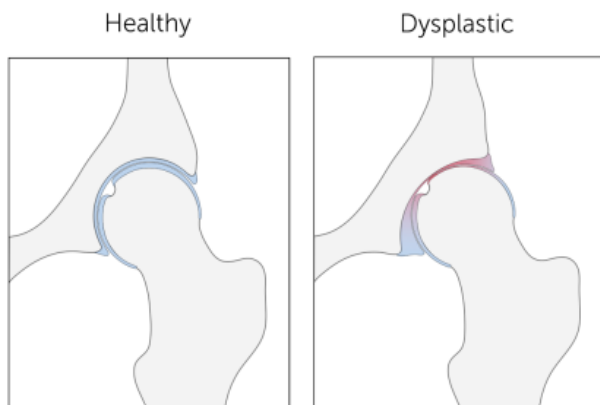


Figure 1: Healthy vs dysplastic hip

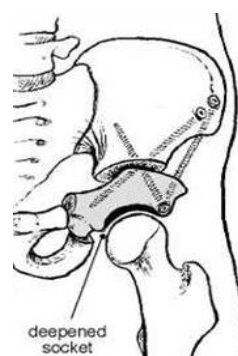


Figure 2: Peri-acetabular osteotomy



Figure 3: Shelf arthroplasty.

Before the widespread use of the PAO, a less technically demanding and less invasive surgical procedure called shelf arthroplasty was commonly performed. (5,6) The shelf arthroplasty technique was described by König et al. in 1891. (7) In this procedure, a bone graft is placed above the hip joint to increase the coverage of the femoral head (Figure 3). However, there are concerns associated with shelf arthroplasty. The placement of the graft must be precise to avoid complications. If the graft is placed too high, it may resorb, and if placed too low, it can cause damage to the cartilage of the joint. (8) Additionally, the quality of the graft material must be sufficient to bear the load and provide long-term stability. (9,10)

Similar to humans, hip dysplasia can also occur in canines and can lead to laxity of the hind legs and AO. Surgical treatment options for canines also include PAO and acetabular shelf arthroplasty. (11)

## 1.2 Technical background

Advancements in technology have revolutionized the manufacturing of acetabular shelf grafts used to treat hip dysplasia, employing CAD/CAM techniques, including 3D (three-dimensional) printing. This modern approach brings several advantages over traditional autologous graft harvesting. By leveraging pre-operative computerized tomography (CT) scans, each implant can be custom-made for the individual patient. This ensures a perfect fit and eliminating the necessity for graft harvesting and reshaping during surgery. (12)

Preliminary results from a cadaveric study conducted at the University Medical Centre Utrecht have indicated difficulties in accurately placing these 3D printed acetabular implants when compared to the pre-operative plan. One of the hypotheses is that it is difficult to feel the correct fit of the implant during surgery. This might be caused by synovial inflammation, a pathological characteristic of OA which causes hypertrophy of the joint capsule. (13) A similar challenge has been observed in the treatment of dysplastic dog patients using 3D printed acetabular roof implants at the Veterinary Faculty of Utrecht University. Consequently, the standard protocol for the dog patients now involves intra-operative verification of the implant position using 2D fluoroscopy, which involves projecting X-ray images onto a 2D screen.

Analysing a 3D structure using 2D fluoroscopy images can be challenging, especially when there is overprojection of an implant on the contralateral side (Figure 4). Besides, the use of radiation should be minimized in accordance with the ALARA principle (As Low As Reasonably Achievable) for radiation exposure to both the patient and surgical staff. To address these issues, Extended Reality (XR) guidance, specifically Augmented Reality (AR) and Mixed Reality (MR), is being explored as an alternative guidance method to place the implants. AR/MR technologies superimpose virtual objects onto the real-world environment, allowing surgeons to visualize the 3D pre-operative planning and the implant's intended location directly on the patient's anatomy.



*Figure 4: Overprojection of canine acetabular roof implants on 2D X-ray makes it challenging to confirm the correct location of the implants.*

By using AR/MR-guidance, real-time information about the position of instruments and implants relative to the planned position can be provided. This can improve surgical accuracy and potentially reduce surgical time. The real-time information is often provided to the surgeon via a head-mounted AR/MR headset. Besides, this approach may offer a solution to the challenges associated with analysing 3D structures using 2D fluoroscopy images and reduce radiation exposure during the procedure. (14)

To use AR/MR for surgical navigation, it is necessary to superimpose the virtual content accurately on the correct location within the patient. The spatial relationship between the patient and the AR/MR display must be determined. This process is called 'patient registration'. There are various approaches to perform the patient registration process for orthopedic surgical guidance, including manual alignment, point-based registration, fiducial registration, surface registration, and markerless registration. (15-17) After the patient registration the planned position of implants and/or instruments can be seen as holograms through the head-mounted headset.

The AR/MR software of HoloMA (version 1.3, ICB-M, Sofia, Bulgaria) for was used in this study. The first version of this novel application was released in September 2022 and is compatible with the Microsoft HoloLens 2 head-mounted headset (Microsoft, Redmond, Washington, United States of America). HoloMA's patient registration algorithm makes use of the surface geometry of the bone to determine where the holograms should be positioned in space. This is accomplished by creating a digital point cloud of the bony surface by tracking of a planar black-and-white fiducial of 3.5x3.5 cm (Figure 5). The location of the fiducial is determined through image-analysis. These images are captured via the RGB-camera of the HoloLens 2. Similarly, surgical instruments can be tracked for navigation if equipped with the fiducials. Navigational guidance is established by providing the user directions how to position the instrument.

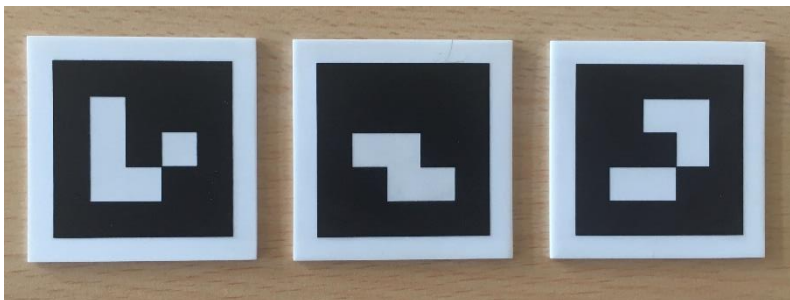


Figure 5: HoloMA fiducials for tracking.

HoloMA was used to position canine 3D printed acetabular roof implants. These implants were designed patient-specifically following a pre-existing automatic workflow in Materialise 3-Matic (17.0, Materialise NV, Leuven, Belgium). The implants were attached to the body of the ilium with four threaded holes for fixation with bicortical locking screws (Figure 6). The implants consisted of an acetabular roof extension and a ventral ilium flange, which improved positioning and stabilizing of the implant. (12,18)

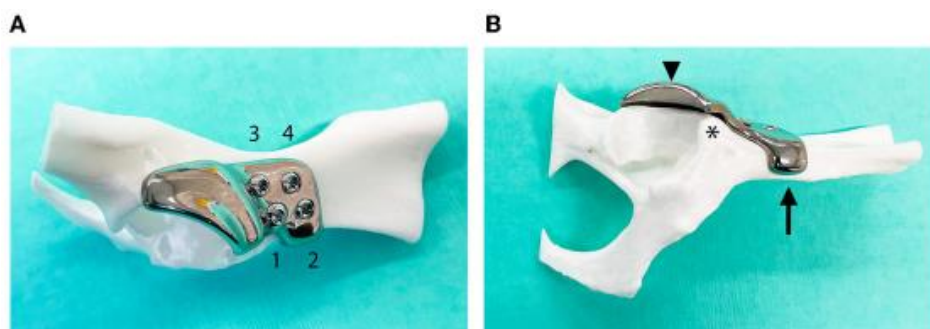


Figure 6: Personalized acetabular roof implant. A) The implant is fixated using four bicortical locking screws. B) The acetabular roof extension (▼) and the ilium flange (↑).

### 1.3 Research aim

The main goal of this project was to determine the AR/MR-guided positioning accuracy of patient-specific acetabular roof implants. To this extend, the novel AR/MR application HoloMA will be used on a Microsoft HoloLens 2. To date, no studies using the HoloMA software have been conducted. The acetabular roof implants are ideally placed with a deviation of less than 1 mm and without rotation relative to the pre-operative plan. Based on literature, a maximum translation error of 4.0 mm and a maximum angulation error of 5.0° was accepted for this pilot study investigating the accuracy of AR/MR-guided surgery. (19)

### 1.4 Thesis outline

This thesis consists of three sections: Patient registration (chapter 2), Surgical navigation (chapter 3) and Implant position accuracy (chapter 4) (Figure 7).

- Patient registration: Patient registration refers to the process of aligning the AR/MR holographic image to the patient. To be able to use the patient registration technique of HoloMA, a tool had to be designed and manufactured. An in silico test was conducted to test the HoloMA patient registration algorithm given the bony surface that is available during the acetabular roof surgical procedure.
- Surgical navigation: After performing the AR/MR patient registration, the user gets navigational instructions via the AR/MR headset where to place the implant. A dedicated tool which holds a tracking fiducial had to be designed and manufactured specifically for the personalized acetabular roof implants.
- Implant position accuracy: Implant placement using the AR/MR surgical navigation was first deployed on phantoms and was followed by a test on a cadaver and in a in vivo dog patient. The accuracy of the implant placement was determined by calculating the translational and angulation error relative to the planned position of the implant.

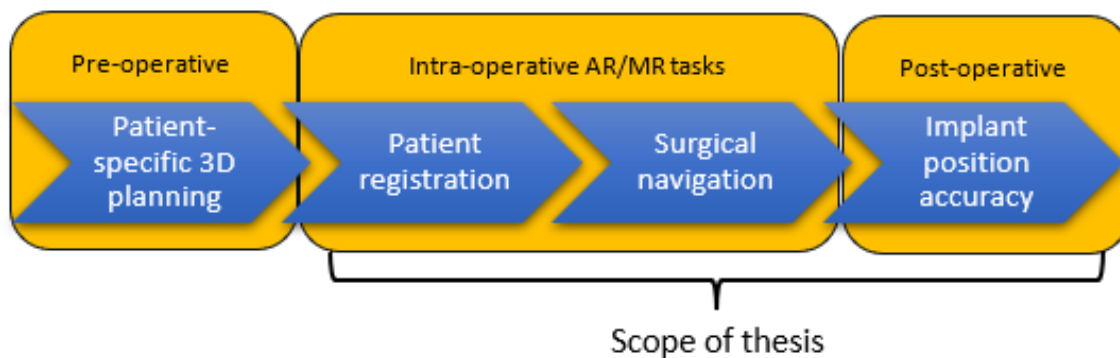


Figure 7: Thesis outline.

## 2 Patient registration

### 2.1 Introduction

To employ AR/MR for surgical navigation, it is necessary to first accurately superimpose the holographic 3D models onto the correct location within the patient. The spatial relationship between the patient and the AR/MR display must be determined. This process is referred to as 'patient registration'.

The built-in patient registration technique of HoloMA relies on the digitalization of the surface of the bony anatomy. The user generates a point cloud which represents the surface of the bone. This is accomplished by continuously tracking a black-and-white fiducial while 'scratching' it against the bony surface. The holographic 3D model of the bone's surface is then aligned with this point cloud to finalize the patient registration. Once the patient registration process is completed, patient-specific holographic models are automatically superimposed onto the patient's actual bone (Figure 8).

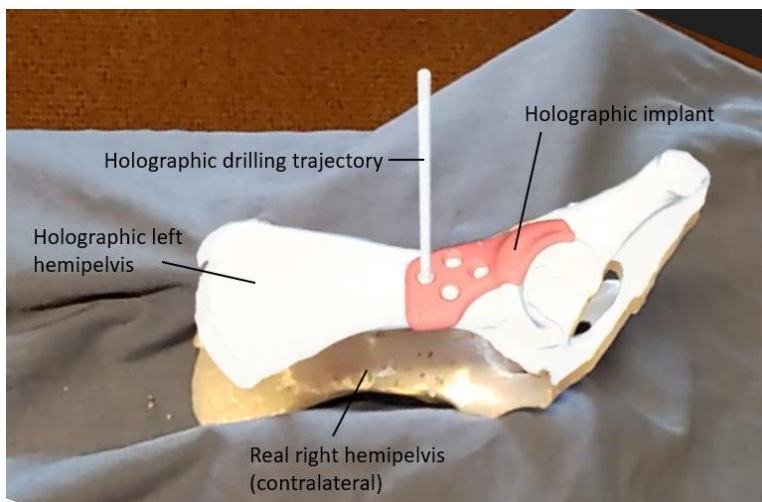


Figure 8: Patient registration result. The holographic left hemipelvis is superimposed to the phantom along with the holograms of the implant and one of the drilling trajectories.

In this chapter, a tool to perform the patient registration process is designed first. Second, an in silico patient registration test is conducted to assess the suitability of the bony surface available during the surgery for achieving an accurate patient registration result.

### 2.2 Methods

#### Registration tool

The AR/MR patient registration process involves digitalizing the bony surface using a fiducial. However, direct access to the canine iliac bone is hindered by surrounding soft tissue. Therefore, a dedicated registration tool which holds the fiducial had to be designed to perform the patient registration process. This was done following a set of design- and performance criteria (Table 1).

Table 1: Design and performance criteria for registration tool.

	Requirement	Rationale
A	Fiducial visible from different orientations.	The user must have the freedom to execute the task from different positions, thus obstruction of the fiducial should be minimized.
B	Stable connection between elements.	A stable connection between different parts of the tool is necessary because the dimensions between the fiducial and tip of the tool is pre-planned.
C	Fiducial outside surgical wound (minimal distance 8.0 cm from tip of tool).	The surgical field is relatively small, so it is preferred to have the fiducial outside the surgical field to avoid collision with the soft tissue.
D	Fiducial orientated perpendicular to user's line of sight.	This will result in the most accurate tracking to determine the location of the fiducial in space.
E	Sterilizable.	The materials must be sterilizable to be used in in vivo scenarios. The design should not contain cavities and/or areas that are hard to clean.
F	Non-flexible parts.	The elements should be rigid because the dimensions between the fiducial and tip of the tool is pre-planned.
G	Tip of tool should be pointy but not sharp.	The tip of the tool should be pointy to guarantee that only the very end of the tip can be in contact with the bone. At the same time, the tip must be blunt avoid injury to the user and/or patient.

After manufacturing the registration tool, the tool was evaluated to ensure it met the design and performance criteria.

#### Defining the registration area

To increase the likelihood of obtaining a correct patient registration result, information about the surface of the iliac bone which is accessible intra-operatively was provided to the HoloMA algorithm. This patient-specific information allows the patient registration algorithm to focus on a specific area for point cloud matching.

The registration area for the acetabular roof implant surgery was determined by estimating the extent of intra-operatively palpable iliac bone around the fixated implant in several dog patients. The following borders of the registration area were defined in collaboration with a board-certified veterinary orthopaedic surgeon (Figure 9):

- Cranial border: Maximum 5 mm beyond the implant's border.
- Dorsal border: Limited to the lateral side of the ilium. The ischium is inaccessible due to the biceps femoris muscle.
- Caudal border: Extends until the capsular tissue of the acetabular rim.
- Ventral border: Encompasses half of the ventral side of the ilium around the ventral flange of the implant, as well as the bony prominence of the rectus femoris attachment.

Indication of the patient-specific registration area on the digital 3D model of the pelvis was performed in Blender (3.1, Blender Foundation, Amsterdam, The Netherlands). This was achieved by selecting the relevant surface and saving it as a separate digital model. This patient-specific 3D model of the registration area was uploaded to the HoloMA software, along with the 3D model of the full bone to perform the patient registration.

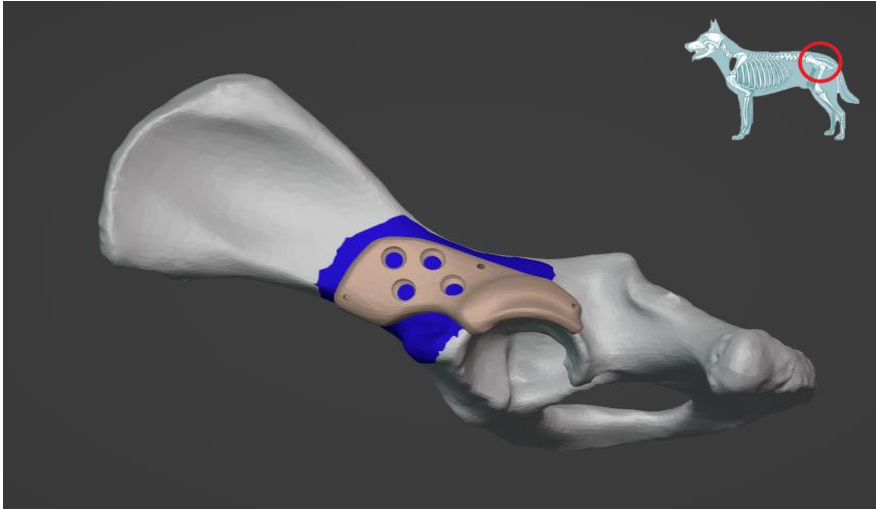


Figure 9: The registration area (blue) is the bony surface which is accessible intra-operatively.

#### In silico patient registration test

The In Silico Patient Registration (ISPR) application of HoloMA was employed to assess the accuracy of the patient registration algorithm when using the defined registration area. The ISPR application randomly selects a user-defined number of points within the registration area to perform the virtual patient registration. The user also has to specify the initial angulation between the source and target, as well as the maximum noise level added to the selected points.

Initially, the in silico patient registration test was performed using 150 collected points, an initial angulation between the 3D model and target of 10°, and a maximum level of noise of 1.5 mm (Table 2). The ISPR application automatically calculated the translational and angulation errors after each patient registration. The test was repeated 100 times using the same registration area. The mean of the translational and angulation error was calculated.

Additionally, the in silico patient registration was also conducted using different values for the number of collected points (50 and 250), initial angulation error (5° and 15°), and a maximum noise level (0.5 mm and 2.5 mm) to analyse the impact of each parameter on the translational and angulation errors. Each variation was repeated 100 times using the same registration area.

Table 2: Test values for in silico patient registration test. ISPR: In Silico Patient Registration, AR: Augmented Reality, MR: Mixed Reality.

ISPR parameter	Primary test value	Rationale	Additional test values
Number of collected points	150	It is assumed that 10 seconds is a reasonable timeframe to reach all sections of the registration area using the registration tool. The HoloMA AR/MR software can locate the fiducial with a rate of approximately 15 per second, so in 10 seconds 150 points can be collected.	50, 250
Initial angulation of 3D model to target	10°	It is assumed that the user can manually align the virtual 3D model with an angulation error of 10° relative to the real object.	5°, 15°
Maximum level of noise	1.5 mm	It is assumed that the fiducial can be located with a maximum error of 1.5 mm, based on the specifications of the HoloMA AR/MR software.	0.5 mm, 2.5 mm

IBM SPSS Statistics (version 29.0, ICM Corp, New York, United States of America) was used to perform the Mann-Whitney U test with Bonferroni correction. This was done to determine if the variations had led to a significant difference in translational error and angulation error relative to results of the primary in silico patient registration test ( $p < 0.05$ ).

## 2.3 Results

### Registration tool

The resulting registration tool consisted of two parts: a pin and a fiducial holder (Figure 10). Both parts were designed and manufactured in-house. The pin was fabricated from stainless steel using CNC milling. The fiducial holder was 3D printed in nylon with a *Formlabs Fuse 1+ 30W* selective laser sintering printer (Formlabs, Somerville, MA, USA). The pin, located at the centre of the fiducial, could be unscrewed from the fiducial holder. The fiducial fitted tightly between the sliding grooves of the fiducial holder. Key dimensions of the registration tool components are provided in Figure 11.

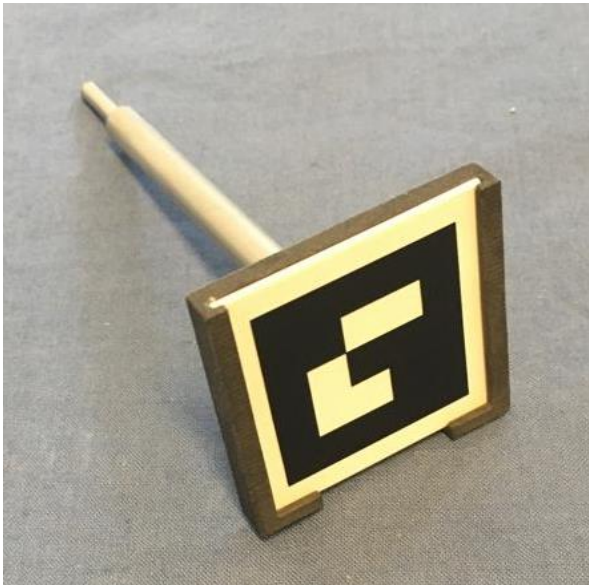


*Figure 10: Assembled registration tool with fiducial marker.*

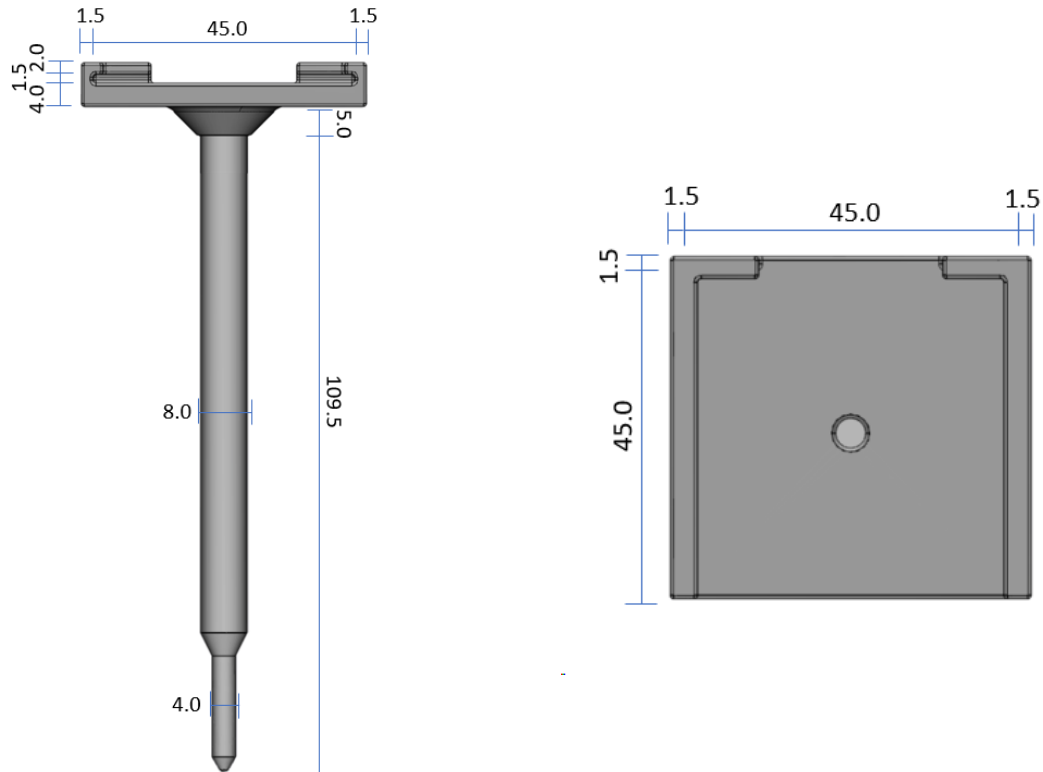


Figure 11: Key dimensions of the registration tool. All measurements are in millimeters. Left: front view, Right: top view.

All design and performance criteria for the registration tool were met. The evaluation per criteria can be found in Table 3.

Table 3: Evaluation of registration tool.

	Requirement	Requirement fulfilled?	Evaluation
A	Fiducial visible from different orientations.	+	There are no elements that can potentially block the line of sight between the user and fiducial.
B	Stable connection between elements.	+	The fiducial fits tightly between the sliding grooves of the fiducial holder. The pin is secured to the fiducial holder via a screw thread.
C	Fiducial outside surgical wound (minimal distance 8.0 cm from tip of tool).	+	The fiducial is positioned 12.0 cm from the tip of the tool. This allows the user to hold the registration tool like a pen.
D	Fiducial orientated perpendicular to user's line of sight.	+	It is possible to orientate the fiducial perpendicular to the user's line of sight. However, it should be noted that this will block the view on the tip of the tool.
E	Sterilizable.	+	The materials (stainless steel and nylon) are sterilizable. There are no cavities or areas that are hard to clean.
F	Non-flexible parts.	+	The stainless steel pin and the nylon fiducial holder did not show deformations under normal working forces.
G	Tip of tool should be pointy but not be sharp.	+	The tip of the tool will not cause injury to the user or patient under normal working circumstances.

### In silico patient registration test

The mean translational error obtained from the in primary silico patient registration test (150 collected points, 10° initial angulation error and maximum 1.5 mm noise) was  $0.94 \pm 0.23$  mm. The mean angulation error was  $2.49 \pm 0.34^\circ$ .

When 50 points were collected, the translational error significantly increased to  $1.53 \pm 0.75$  mm and the angulation error significantly increased to  $3.45 \pm 1.51^\circ$ . When 250 points were collected, the translational and angulation error both significantly decreased to  $0.66 \pm 0.08$  mm and  $1.10 \pm 0.29^\circ$ , respectively (Table 4, Figure 12).

Table 4: Influence of number of collected points on translational and angulation error.

Test value	n	Mean $\pm$ SD	p-value
<b>150 points</b> - Translation error - Angulation error	100	$0.94 \pm 0.23$ mm $2.49 \pm 0.34^\circ$	
<b>50 points</b> - Translation error - Angulation error	100	$1.53 \pm 0.75$ mm $3.45 \pm 1.51^\circ$	<0.001 <0.001
<b>250 points</b> - Translation error - Angulation error	100	$0.66 \pm 0.08$ mm $1.10 \pm 0.29^\circ$	<0.001 <0.001

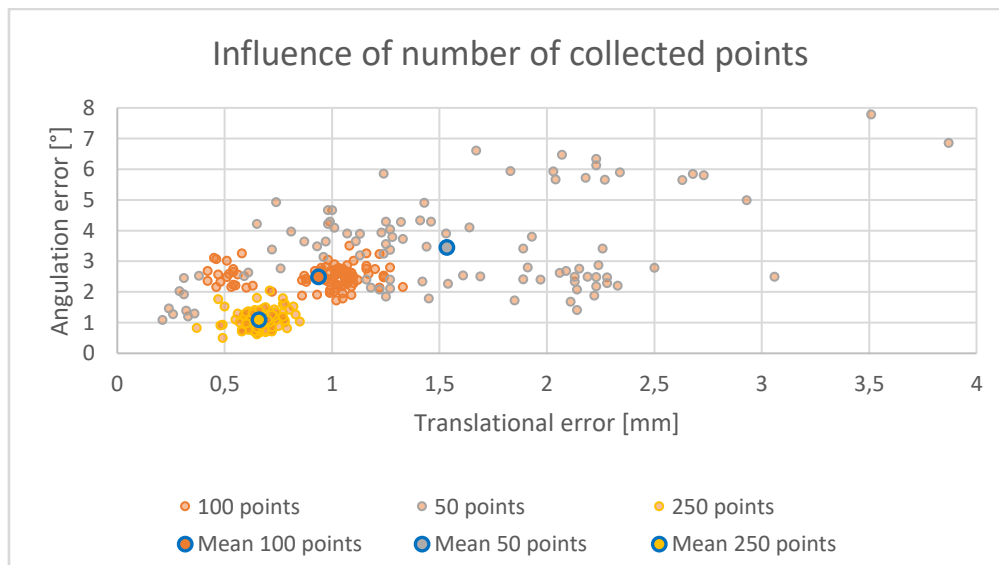


Figure 12: Influence of number of collected points on translational and angulation error.

When an initial angulation error of  $5^\circ$  was used, the translational error significantly increased to  $1.30 \pm 0.10$  mm and the angulation error significantly decreased to  $0.81 \pm 0.27^\circ$ . With an initial angulation error of  $15^\circ$ , the translational and angulation error both significantly increased to  $1.60 \pm 0.78$  mm and  $3.18 \pm 0.58^\circ$ , respectively (Table 5, Figure 13).

Table 5: Influence of initial angulation on translational and angulation error.

Test value	n	Mean ± SD	p-value
10° - Translation error - Angulation error	100	0.94 ± 0.23 mm 2.49 ± 0.34°	
5° - Translation error - Angulation error	100	1.30 ± 0.10 mm 0.81 ± 0.27°	<0.001 <0.001
15° - Translation error - Angulation error	100	1.60 ± 0.78 mm 3.18 ± 0.58°	<0.001 <0.001

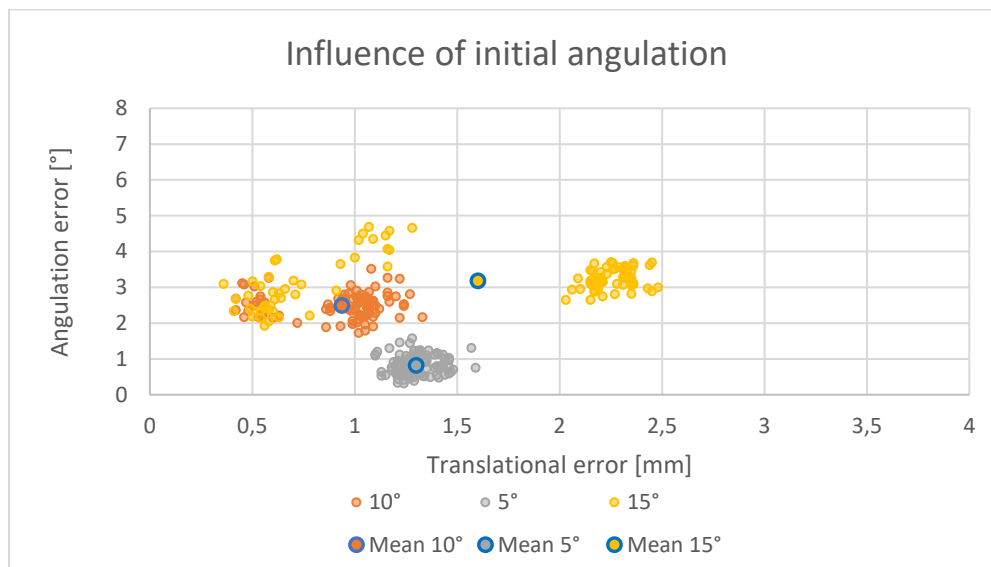


Figure 13: Influence of initial angulation on translational and angulation error.

When a maximum level of noise of 0.5 mm was used, the translational error significantly decreased to  $0.67 \pm 0.11$  mm and the angulation error significantly increased to  $3.60 \pm 0.24^\circ$ . When an initial angulation error of  $15^\circ$  was used, the translational and angulation error both significantly increased to  $1.55 \pm 0.81$  mm and  $3.80 \pm 1.18^\circ$ , respectively (Table 6, Figure 14).

Table 6: Influence of noise on translational and angulation error.

Test value	n	Mean ± SD	p-value
1.5 mm - Translation error - Angulation error	100	0.94 ± 0.23 mm 2.49 ± 0.34°	
0.5 mm - Translation error - Angulation error	100	0.67 ± 0.11 mm 3.60 ± 0.24°	<0.001 <0.001
2.5 mm - Translation error - Angulation error	100	1.55 ± 0.81 mm 3.80 ± 1.18°	<0.001 <0.001

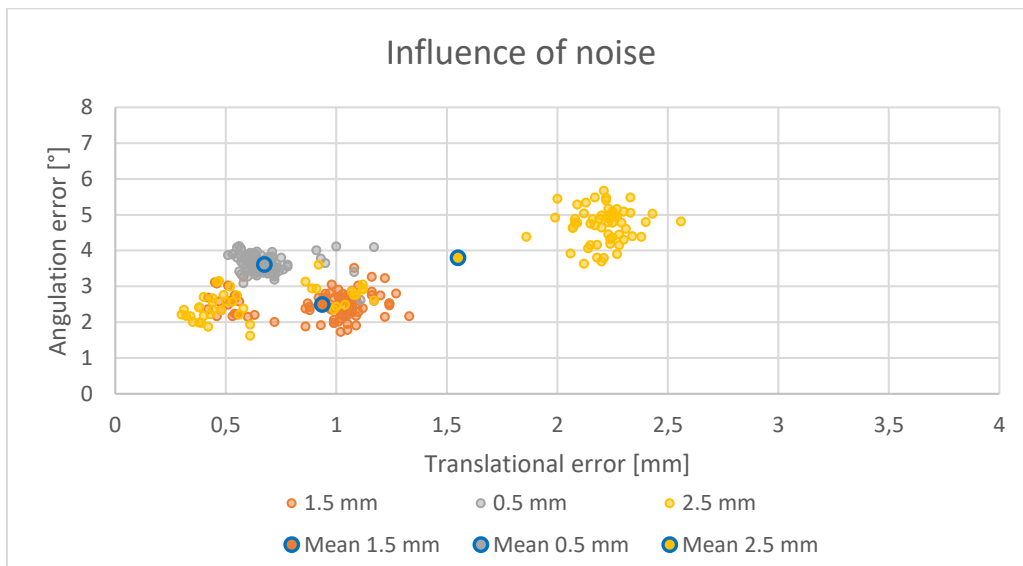


Figure 14: Influence of noise on translational and angulation error.

## 2.4 Discussion

### Summary

A stable tool to perform the patient registration was successfully designed and manufactured. Following the definition of the intra-operatively accessible iliac bone surface (registration area), an *in silico* patient registration test was conducted to assess HoloMA's patient registration accuracy in positioning the 3D model correctly. The results showed a mean translational error of  $0.94 \pm 0.23$  mm and a mean angulation error of  $2.49 \pm 0.34^\circ$ . These results align with the priorly defined goal of this project (maximum translation error of 4.0 mm and maximum angulation error of  $5.0^\circ$ ).

### Limitations and recommendations: in vivo patient registration

It is crucial to note that the results presented above were obtained using specific parameters, including 150 collected points, an initial angulation error of  $10^\circ$ , and a maximum noise level of 1.5 mm. When variations in these parameters were introduced, such as fewer collected points (50), an increased initial angle ( $15^\circ$ ), or a higher maximum noise level (2.5 mm), both the translational and angulation errors increased significantly as expected. However, an unexpected observation emerged when the initial angulation error was reduced to  $5^\circ$ : only the angulation error significantly decreased, while the translational error significantly increased. A similar pattern was observed when the noise level was reduced to 0.5 mm, resulting in a significant decrease in translational error but a significant increase in angulation error. The underlying causes of these contradictory results remain unexplained. It is imperative to delve deeper into these phenomena through further investigation, examining whether they persist across different subjects or in alternative surgical procedures.

The results of the *in silico* patient registration test for the acetabular roof surgical procedure are promising, especially when many points can be collected. However, it should be noticed that the ISPR application selects points from the entire registration area without considering any intra-operative human factors or clinical constraints. During the actual surgery, scenarios may occur in which the user can not fully adhere to the predefined registration area. Some sections may remain inaccessible, or there could be more bony surface available than initially indicated within the registration area. Presently, we lack an understanding of how the patient registration algorithm responds when the point cloud is collected from only a part of the registration area or when points are collected from outside this area.

Furthermore, it should also be noted that the random point selection of the ISPR application does not represent a realistic scenario compared to the intra-operative AR/MR patient registration process. In practise, the user is supposed to continuously collect points. This might lead to clusters of points at certain sections while in other sections the point cloud is less dense. Therefore, it is recommended to be able to simulate this using a user-defined point cloud in the ISPR application. This enables the users to prepare the intra-operative patient registration process more effectively. It would also allow to determine which areas should be emphasised to collect an increased number of points from.

#### Limitations and recommendations: registration tool

The prominent limitation in the current design of the registration tool is regarding the position of the fiducial relative to the tip of the tool. One of the design criteria was to have the fiducial perpendicular to the user's line of sight. However, when the user is performing the patient registration with the fiducial at 90°, the fiducial obstructs the view on the tip of the tool. To resolve this issue, alternative configurations of the fiducial relative to the pen should be explored. Possible solutions include placing the fiducial off-centre or positioning the fiducial on a different angle relative to the pen.

Another limitation concerns the ergonomics of the registration tool. Users are currently required to hold it in a manner resembling a writing pen. However, this design may necessitate the user's hand entering the surgical wound to reach the bony surface with the tool's tip. This can potentially limit the access to certain sections of the registration area. To address this concern, solutions such as lengthening the tool or incorporating a handle to allow the user to hold the tool at an extended distance from the tip should be considered.

## 3 Surgical navigation

### 3.1 Introduction

After patient registration, the AR/MR navigation can be employed to guide users in the precise placement of surgical instruments and implants according to pre-operatively planned positions. HoloMA can locate the tools via a fiducial marker attached to it. Users receive both visual and written instructions through holograms displayed via the HoloLens 2 where to place the instrument (Figure 15).

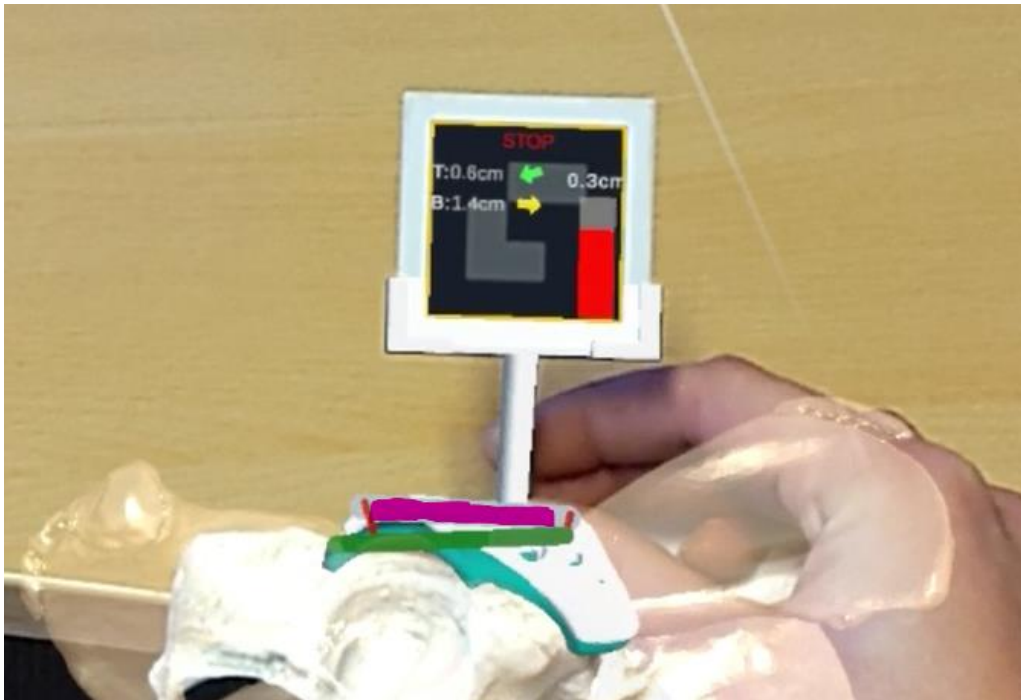


Figure 15: HoloMA AR/MR surgical navigation. The instructions how to align the instrument are provided via written distances superimposed on the fiducial as well as visuals. In this example, the user had to position the pink cylinder (real) to the green cylinder (virtual).

In this chapter, a tool to affix the fiducial marker onto the personalized acetabular roof implant was designed to enable localization for the AR/MR surgical navigation guidance.

### 3.2 Methods

#### Navigation tool

Tracking the personalized acetabular roof implant is accomplished via locating a fiducial attached to it. Therefore, a dedicated navigation tool had to be designed to incorporate the fiducial into the implant. This was done following a set of criteria (Table 7).

Table 7: Design and performance criteria for the surgical navigation tool.

	Requirement	Rationale
A	Fiducial visible from different orientations.	The user must have the freedom to execute the task from different positions, thus obstruction of the fiducial should be minimized.
B	Stable connection between elements.	A stable connection between different parts of the tool is necessary because the dimensions between the fiducial and implant is pre-planned.
C	Fiducial outside surgical wound (minimal 7 cm above implant)	The surgical field is relatively small, so it is preferred to have the fiducial outside the surgical field to avoid collision with the soft tissue.
D	Fiducial orientated perpendicular to line of sight	This will result in the most accurate tracking to determine the location of the fiducial in space.
E	Sterilizable	The materials must be sterilizable to be used in in vivo cases. The tool should not contain cavities and/or areas that are hard to clean.
F	Non-flexible parts	The elements should be rigid because the dimensions between the fiducial and tip of the tool is pre-planned.
G	Fiducial should not obstruct the drill trajectory	The fiducial remains attached to the implant during drilling the screw tunnels, thus the drilling trajectory should be accessible. The drilling of the tunnels is executed using a drill guide.
H	Universal application	The tool should fit on all personalized acetabular roof implants.

Regarding the use of the drill guides (requirement G), the following scenarios were considered:

- 1) Availability of an 8.0 cm metallic drill guide (classified prototype)
- 2) Availability of a 3.5 cm metallic drill guide (Figure 16)



Figure 16: Metallic drill guide of approximately 3.5 cm.

After manufacturing the (different versions of the) navigation tool, the tool was evaluated if the design and performance criteria were met.

### 3.3 Results

#### Scenario 1: 8.0 cm drill guide

The resulting navigation tool for use with the 8.0 cm drill guide is a fiducial holder which can slide over the top of the drill guide (Figure 17). The sliding part features a complementary pattern to the drill guide's top. The fiducial holder was 3D-printed in nylon using a *Formlabs Fuse 1+ 30W* printer. Key dimensions of the navigation tool components are provided in Figure 18.



Figure 17: Navigation tool including the fiducial attached to the implant via an 8.0 cm drill guide (scenario 1). The drill is inserted in the drill guide.

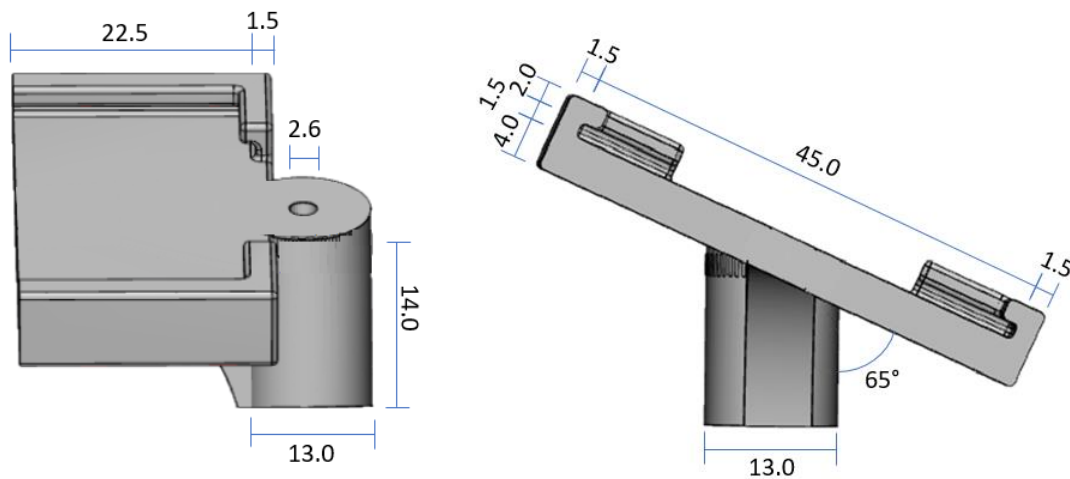


Figure 18: Key dimensions of navigation tool for scenario 1 (8.0 cm drill guide). All measurements are in millimeters, unless stated else. Left: front view. Right: side view.

#### Scenario 2: 3.5 cm drill guide

The resulting navigation tool for use with the 3.5 cm drill guide is a fiducial holder attached to a hollow cylinder (Figure 20). The upper part of the cylinder serves as an extension of the metallic drill guide, with an appropriate inner diameter to guide the drill. The lower part can slide over the metallic drill guide. The fiducial holder and cylinder were 3D-printed as a single part in nylon using a Formlabs Fuse 1+ 30W printer. Key dimensions of the navigation tool components are provided in Figure 19.



Figure 19: Navigation tool to be used in combination with the 3.5 cm drill guide. The lower part contains the part that slides over the metallic drill guide.

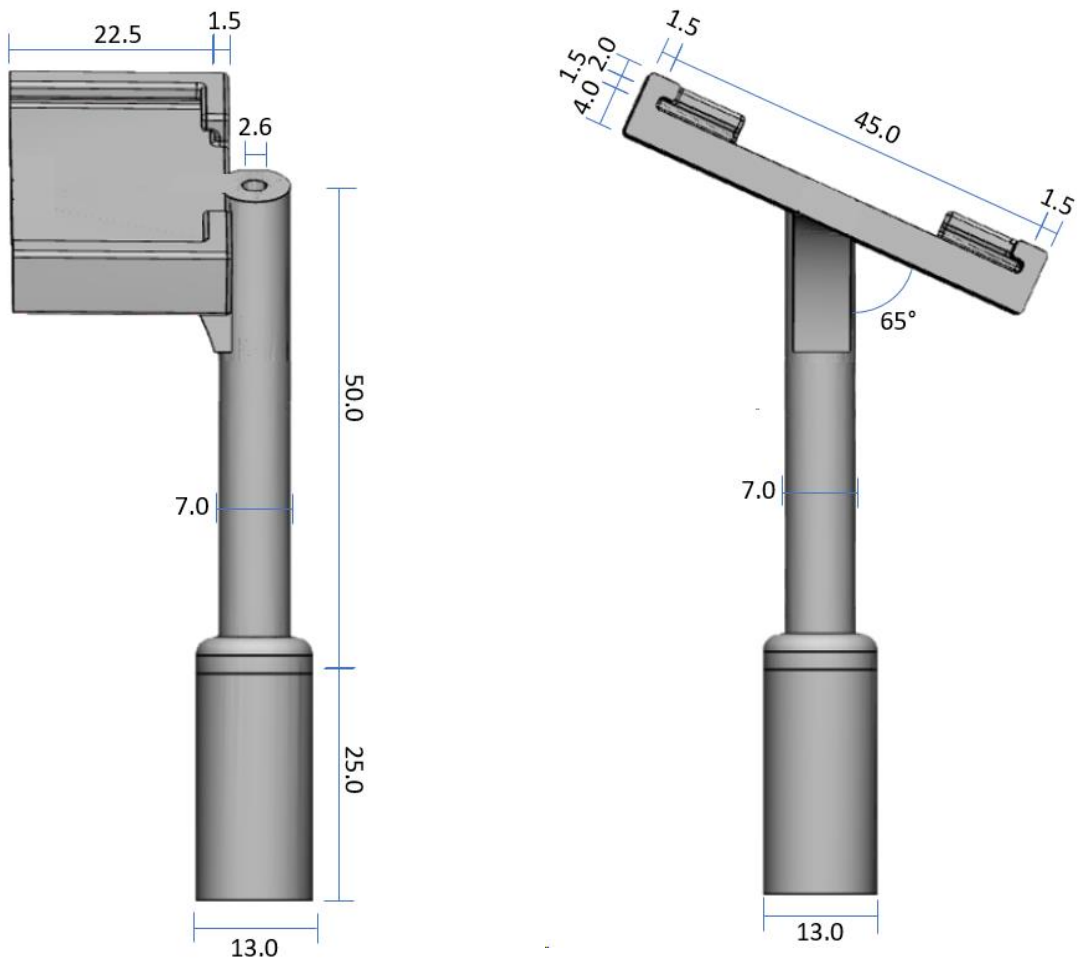


Figure 20: Key dimensions of navigation tool for scenario 2 (3.5 cm drill guide). All measurements are in millimeters, unless stated else. Left: front view. Right: side view.

The evaluation of both navigation tools against the criteria is presented in Table 8. All requirements were fulfilled, except for requirement B.

Table 8: Evaluation of the navigation tools.

	Requirement	Requirement fulfilled?		Evaluation
		8.0 cm	3.5 cm	
A	Fiducial visible from different orientations.	+	+	In the current design with the fiducial positioned on the left side of the drill guide, the drill can potentially be in the line of sight between the user and the fiducial if the user is operating the drill with the left hand. Therefore, a mirrored version is also manufactured so the fiducial is on the right side of the drill.
B	Stable connection between elements.	-	-	8.0 cm: The fiducial holder fits tightly over the pattern of the 8 cm drill guide and can not rotate. The location of the fiducial is however dependent on the torque used to fasten the drill guide. 3.0 cm: The part that slides over the 3 cm drill guide fits tightly, but due to the cylindrical shape it still has the potential to rotate around the axis of the drill guide.
C	Fiducial outside surgical wound (minimal 7 cm above implant)	+	+	The fiducial is positioned at 7.0 cm from the implant .
D	Fiducial orientated perpendicular to line of sight	+	+	The fiducial is positioned at 65° relative to the drill so it faces towards the user when the acetabular roof implant is at working height.
E	Sterilizable	+/-	+/-	The navigational tools were made of nylon, which is sterilizable. However, the parts that slide over the drill guides might be hard to clean.
F	Non-flexible parts	+	+	The navigational tools did not show deformations under normal working forces.
G	Fiducial should not obstruct the drill trajectory	+	+	The fiducial is positioned alongside the drill guide so it does not obstruct the drill trajectory.
H	Universal application	+	+	The navigation tool is not patient-specific.

### 3.4 Discussion

#### Summary

Two tools were designed and manufactured to enable AR/MR surgical navigation for personalized acetabular roof implants. The first is intended for use in combination with an 8.0 cm drill guide, while the second is designed for a 3.5 cm drill guide.

#### Limitations and recommendations

In the current design of both navigation tools, the fiducial holder is mounted to the drill guide, but the fiducial's location in respect to the implant can still vary (requirement B not fulfilled). In the first scenario, the fiducial holder slides over the grooves of the drill guide, causing its position to depend on the torque used to fasten the drill guide to the implant. In the second scenario, the top of the drill guide is a cylinder without grooves, allowing the navigation tool to rotate around the axis of the drill

guide. A solution to cope with this variation is to equip the drill guide and implant with markings which indicate if the drill guide is in the preplanned position. Additionally, grooves should be added to the top of the 3.5 cm drill guide to prevent the navigation tool from rotating. However, these changes to the design of the implants and drill guides are undesirable.

As a workaround for this project, it was decided to navigate the drill guide to the pre-planned position of the screw tunnels rather than the implant itself. This mitigates uncertainties regarding the fiducial's position relative to the implant but comes with the drawback of not being able to immediately navigate the implant to the correct location. This solution requires navigational AR/MR guidance for drilling at least two screw tunnels to position the implant according to the planning: the first screw to determine the position and the second to determine the rotation in relation to the first screw.

## 4 Implant position accuracy

### 4.1 Introduction

New technologies should be tested thoroughly before the introduction in clinical practise. The AR/MR-guidance of HoloMA using the patient registration (chapter 3) and surgical navigation (chapter 4) is tested in the current chapter as a pilot study.

The goal of this pilot study is to position the implants with a maximum translational error of 4.0 mm and a maximum angulation error of 5.0° relative to the pre-operatively planned position.

### 4.2 Methods

#### Overview

Accuracy tests using AR/MR-guidance of HoloMA to place personalized acetabular roof implants was conducted in 3 phases, namely:

1. Phantom test
2. Cadaveric test
3. In vivo dog patient test

Pre-operatively, the personalized acetabular implants were manufactured and the patient-specific 3D models for the AR/MR guidance were created. Intra-operatively, the user performed the patient registration and placed the implants according to the AR/MR surgical navigation of HoloMA displayed via a Microsoft HoloLens 2. Post-operatively, the subjects were CT scanned and an analysis was performed to determine the translational and angulation error of the implant relative to the pre-planned position. More details about each section can be found below.

The accuracy results of the implants were reviewed by the veterinary surgeon after each phase. Approval was required to proceed to the next phase.

#### Subjects and implants

For the phantom test, the anatomy of two dog patients with bilateral hip dysplasia and a cadaveric specimen were selected. All subjects underwent pre-operative pelvic CT scans. A 3D printed model of the full pelvis was created using an Ultimaker 3 fusion deposit printer (Ultimaker B.V., Geldermalsen, NL) in polylactic acid (PLA). The infill density of the phantoms was set to 50% with a gyroid pattern to mimic cancellous bone structure. The phantoms were secured using a drill clamp fixed to a table. The personalized implants for the phantom test were 3D printed from resin using a NextDent 5100 digital light processing printer (NextDent B.V., Soesterberg, The Netherlands). Solely for analytical purposes, 3 cylindrical holes ( $\varnothing=2.0$  mm) were designed on the lateral side of each implant. The depth of these cylinders was 2.0 mm. After 3D printing the implants, glass beads ( $\varnothing=2.0$  mm) were fixated in these holes with glue.

For the cadaveric test, one fresh-frozen canine cadaveric specimen was selected. A CT-scan of this specimen was made prior to freezing. After defrosting, the cadaver was stabilized using a vacuum sandbag which was wrapped around the contralateral side of the pelvis. Tape was used for further fixation to the surgical table. The subject was draped before incision. The ilium and hip joint were exposed by performing a tenotomy of the deep gluteal muscle and removal of its attachment to the ilium. The articularis coxae muscle was released. To aid the exposure of the iliac bone, the femur was elevated to be able to lift the gluteus profundus muscle.

The personalized implants for the cadaveric test were 3D printed in Ti-6Al-4V grade 23 using the ProX

DMP 320 direct metal printer (3D Systems, Leuven, Belgium). Similar to the phantom test, 3 cylindrical holes ( $\varnothing=2.0$  mm) were designed on the lateral side of each implant. The depth of these cylinders was now reduced to 1.0 mm for easier distinction between the glass beads and the titanium on the post-operative CT-scan.

For the in vivo dog patient test, one patient with bilateral hip dysplasia was selected. This dog patient was scheduled for surgical treatment of hip dysplasia using personalized acetabular roof implants. A pre-operative CT scan was made as standard protocol for this surgery. During the surgery, the dog patient was stabilized using a vacuum sandbag which was wrapped around the contralateral side of the pelvis. Tape was used for further fixation to the surgical table. The same approach as described for the cadaveric test was used to get to the iliac bone.

The personalized implants for the in vivo dog patient test were 3D printed in Ti-6Al-4V grade 23 using the ProX DMP 320 direct metal printer (3D Systems, Leuven, Belgium).

#### Data preparation for AR/MR tasks

For each subject, a pre-existing file containing the digital 3D models of the pelvic bone and the personalized implants on the planned position was used. These files were priorly generated using an automatic workflow in Materialise 3-Matic for designing the personalized acetabular roof implants.

To be able to perform the patient registration task, the intra-operatively available bony surface of the ilium (registration area) had to be indicated. The borders of this registration area were previously defined in Chapter 2. To be able to perform the surgical navigation, the drilling trajectories had to be determined. This was accomplished by extending the planned screw trajectories laterally in Materialise 3-Matic (Figure 21).

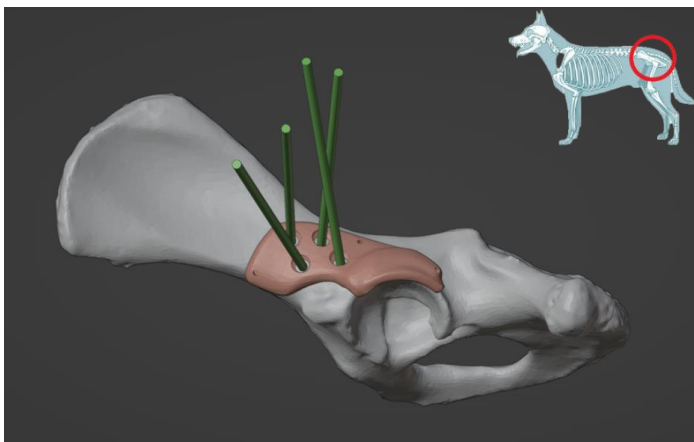


Figure 21: pre-planned implant position (pink) and drilling trajectories (green).

The digital 3D models of the pelvic bone (separated in 2 hemipelves), the implants, the registration areas and the drilling trajectories were uploaded to the HoloLens 2 in .GLB-format.

#### Intra-operative patient registration

The registration tool which was designed in chapter 2 was used to perform the patient registration process (Figure 22). Prior to patient registration, the built-in fiducial depth calibration procedure of HoloMA was performed. This calibration ensured the correct relationship between the fiducial and the registration tool's tip. If necessary, a mock point cloud was collected from the surface of a table to confirm calibration accuracy. The point cloud had to match the surface of the table. Otherwise, fiducial depth calibration and point cloud collection from the table was repeated.

Before obtaining the point cloud of the iliac bone, the user positioned the holographic 3D model of the (hemi)pelvis alongside the real bone in the correct orientation. The user was instructed to create a dense point cloud covering all sections of the registration area, with emphasis on the ventral rim of the ilium and the bony prominence at the insertion site of the rectus femoris muscle.

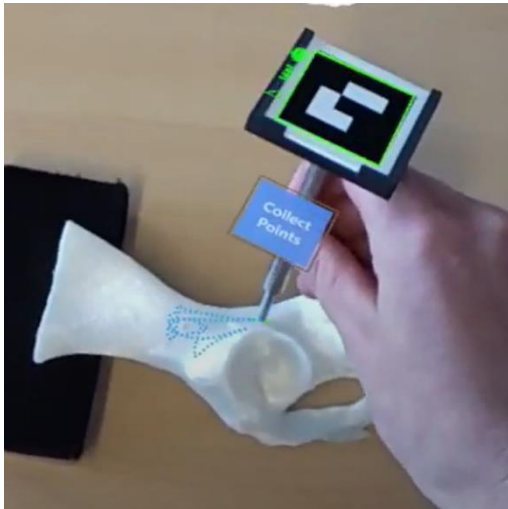


Figure 22: Obtaining the point cloud (blue dots) for the patient registration using the registration tool.

The result of the patient registration process is the superimposing of the holographic model of the bone on the patient anatomy along with the implant and drilling trajectories. If the user was not satisfied with the patient-registration result, the user was allowed to continue collecting more points for the point cloud or discard the current point cloud and restart.

#### Intra-operative surgical navigation

During the phantom test and the cadaver test, the metallic drilling guides were unavailable. Therefore, the 8.0 cm drill guide was reverse-engineered and 3D printed in resin using the NextDent 5100 digital light processing printer. This drill guide was used in combination with the fiducial holder that was placed on top of the drill guide (navigation tool scenario 1, see chapter 3). The 3.5 cm metallic drill was available during the in vivo dog patient test (navigation tool scenario 2, see chapter 3).

The AR/MR surgical navigation workflow consisted of the following steps (Figure 23):

1. The drill guide is screwed to a screw hole of the implant. The navigation tool was mounted to the drill guide so the fiducial is facing towards the user. The user followed holographic directional instructions superimposed on the fiducial of the navigation tool to reach the correct position for drilling (Figure 24).
2. After drilling the first screw tunnel, the drill guide and navigation tool were removed temporarily from the implant to allow loose tightening of the first screw. This secured the implant while allowing slight rotational movement. In the in vivo dog patient test, the implant position was now verified via fluoroscopy by the board-certified veterinary surgeon for safety reasons.
3. The drill guide is screwed to the second screw hole and the navigation tool is mounted to the drill guide, so the fiducial is facing towards the user. The user drilled the second screw tunnel following the navigational instructions.
4. The drill guide and navigation tool were removed from the implant. Both screws are tightened firmly for the definite implant position.

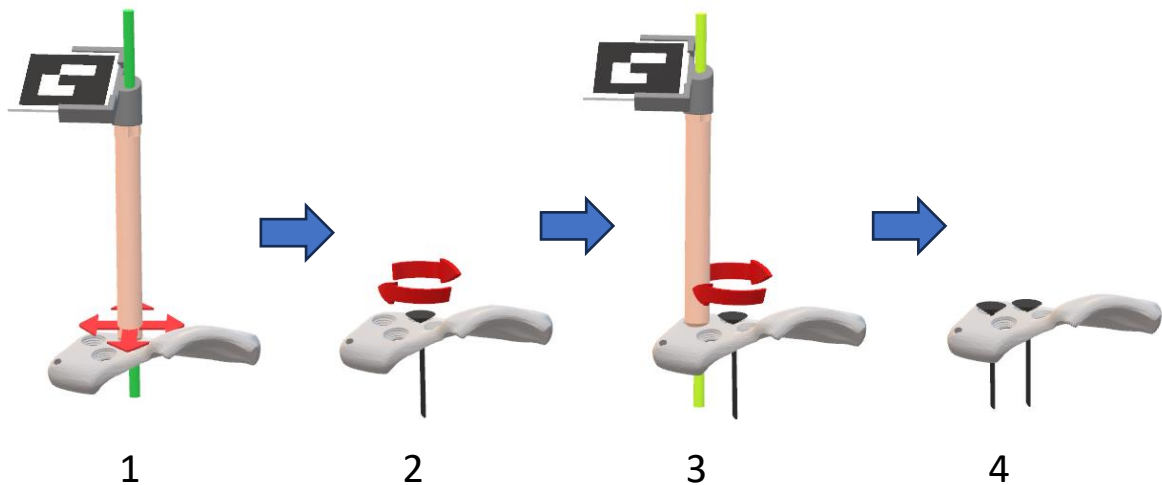


Figure 23: Workflow AR/MR surgical navigation of personalized acetabular roof implants.

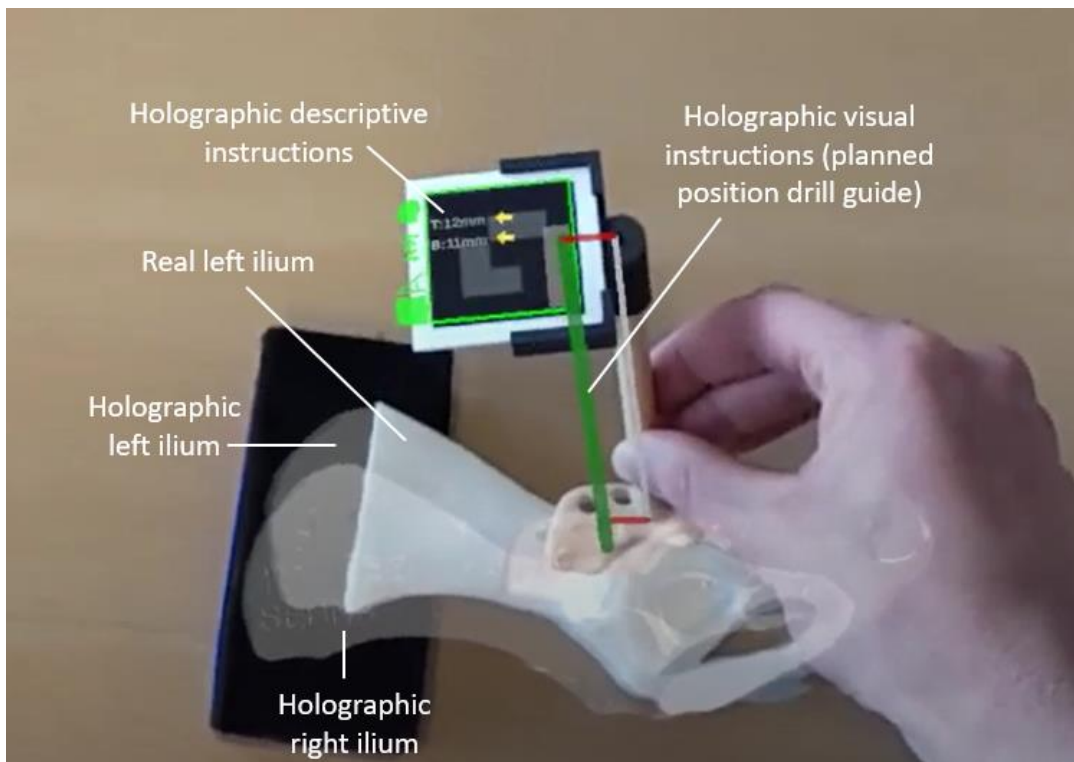


Figure 24: AR/MR-guided surgical navigation. The instructions how to align the instrument are provided via written distances superimposed to the fiducial as well as visuals (green and red lines) along which the drill guide has to be positioned.

#### Accuracy analysis

All phantoms were post-operatively CT scanned using the Brilliance CT Big Bore (Philips Medical Systems Nederland B.V., Best, The Netherlands) with a slice thickness of 0.9 mm. The cadaver and in vivo dog patient were CT scanned immediately post-operative using the SOMATOM Definition AS (Siemens Healthineers AG, Erlangen, Germany) using a slice thickness of 0.6 mm according to the standard protocol for this surgical procedure. Metal artifact reduction was enabled.

Segmentation of the pelvis and implants on the post-operative CT scans was performed semi-automatically in Materialise Mimics (25.0, Materialise, Leuven, Belgium). The glass beads were segmented by placing spheres with a diameter of 2.0 mm at the desired locations on the implant. In

Materialise 3-Matic the post-operative pelvis was registered to the pre-operative pelvis, which was tilted 30° relative to the posterior pelvic plane to mimic a weight-bearing position of the dog (Figure 25).

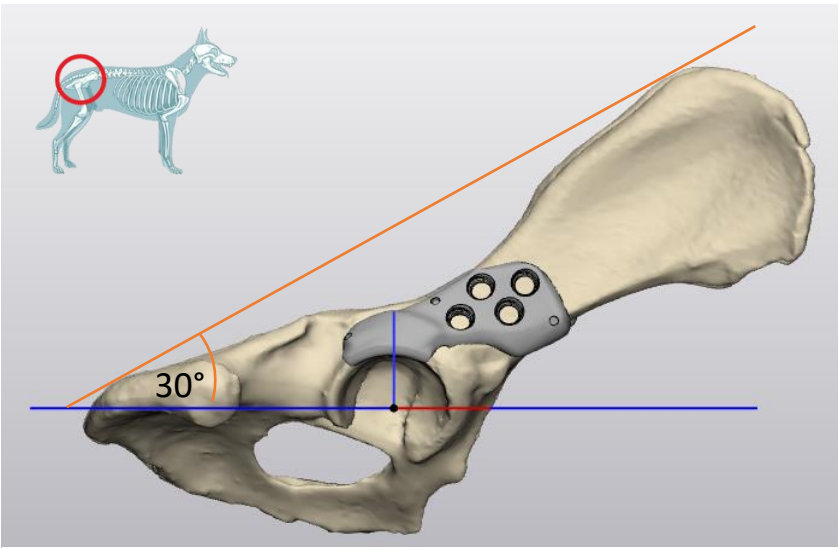


Figure 25: Lateral view of pelvis tilted 30°.

The translational error of the AR/MR-guided implant placement relative to the planned position was determined by calculating the Euclidean distance between corresponding glass beads (Equation 1). Additionally, the Euclidean distance between the isocentre of the AR/MR-guided implant and the planned position was measured. The isocentre was defined as the middle of the three glass beads on the implant (Figure 26).

$$d(p, q) = \sqrt{(p_1 - q_1)^2 + (p_2 - q_2)^2 + (p_3 - q_3)^2}$$

Equation 1: Euclidean distance formula. *p* and *q* are the coordinates of corresponding glass beads.

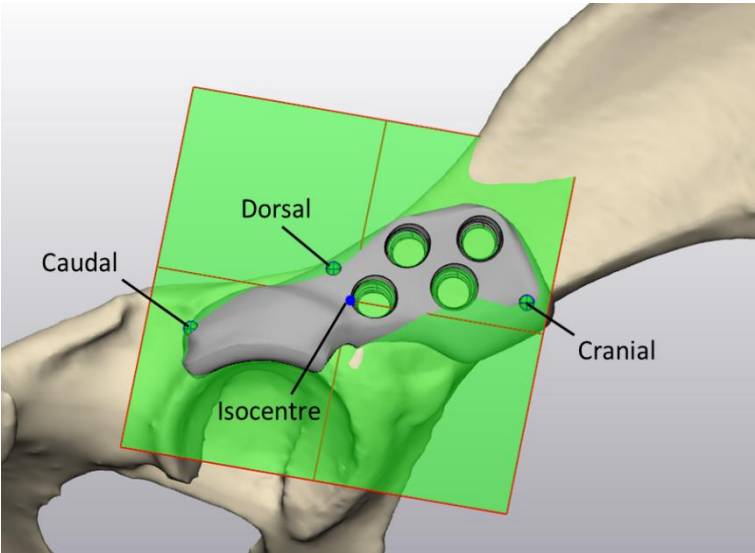


Figure 26: Implant isocentre and naming convention of the glass beads. The plane is spanned through the middle of the beads.

To determine the angular accuracy, a plane was spanned between the 3 glass beads of both the planned and the post-operative implants (Figure 26). The angular error between these planes was measured in the sagittal, transversal, and dorsal anatomical plane with the pelvis oriented in the weightbearing position. The anatomical dorsal plane was defined as the posterior pelvic plane tilted 30° relative to the posterior pelvic plane. The sagittal and transverse planes were set perpendicular to the dorsal plane (Figure 27).

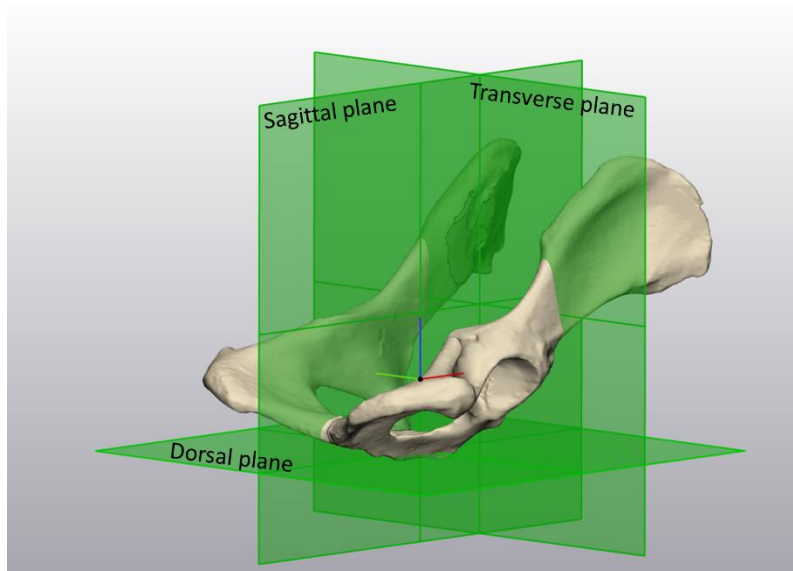


Figure 27: Anatomical planes of the canine pelvis.

### 4.3 Results

Four different subjects were used in this study, with the anatomy of the canine cadaveric specimen being used in both the phantom and cadaveric test. A total 8 implants were positioned using AR/MR-guidance (phantoms = 6, cadaver = 2, in vivo dog patient = 0). The characteristics of the registration area of all subjects are shown in Table 9.

Table 9: Characteristics of the registration area.

Subject	Type	Laterality	No. of mesh faces in registration area	Area of registration area [cm <sup>2</sup> ]	Faces/cm <sup>2</sup> of registration area
A	Phantom	Left	1342	14.55	92.2
		Right	1320	14.76	89.4
B	Phantom	Left	906	10.29	88.1
		Right	804	9.60	83.8
C	Phantom + Cadaver	Left	4648	8.31	559.3
		Right	5095	8.43	604.4
D	In vivo	Left	8513	9.31	914.1
		Right	9306	10.65	873.6

### Phantom test

Six personalised acetabular roof implants were implanted on phantoms. Five of these implants were secured using two screws according to the study protocol. One implant ( $C_p$  right) was fixated with one screw due to a software issue while positioning the navigation tool for the second screw. The planned positions as well as the post-operative positions of the implants of the phantom test can be found in Figure 28. Additional views can be found in Appendix A.

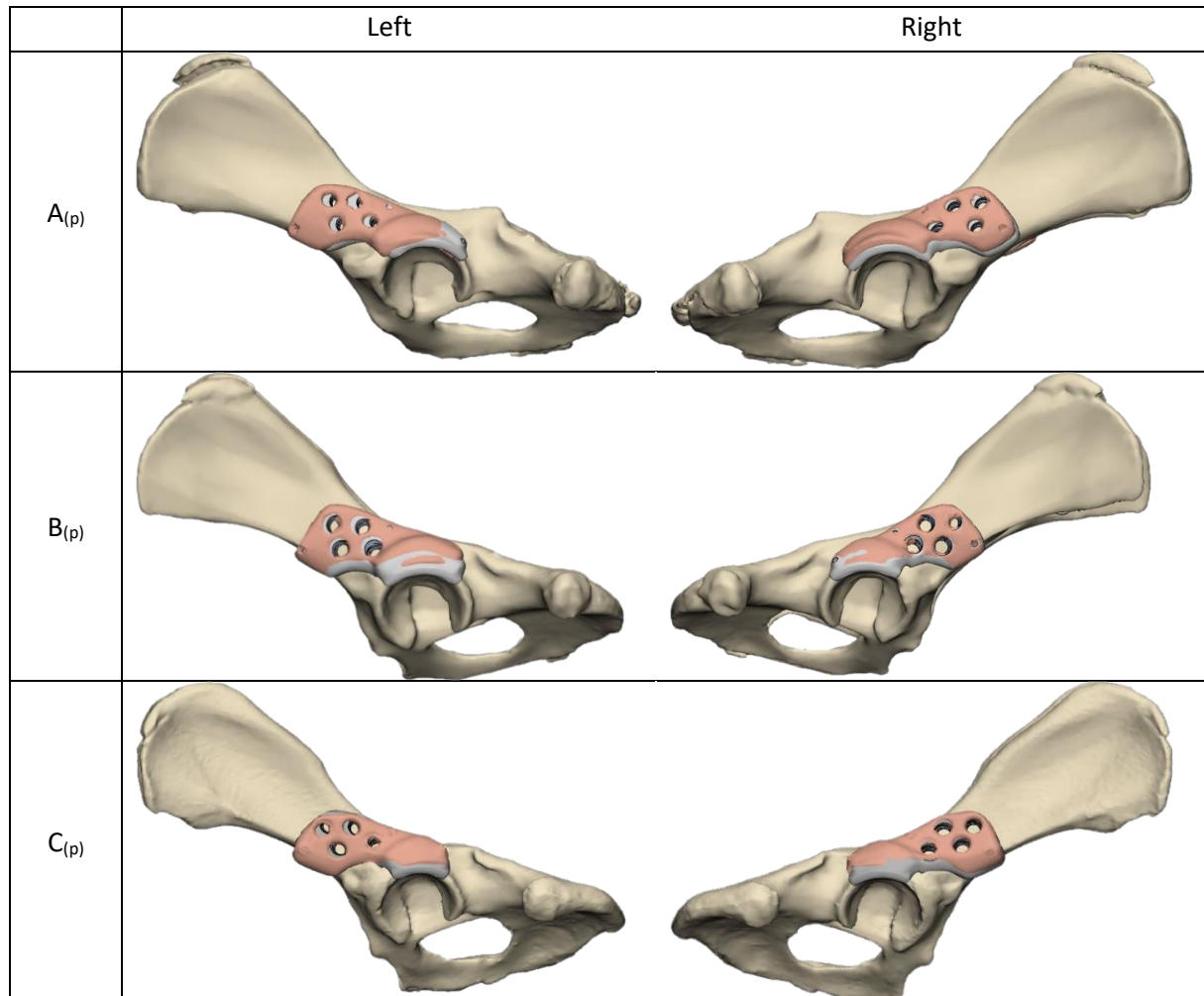


Figure 28: The planned implant positions (gray) and the post-operative implant positions (pink) of the phantom test.

The translational errors of the implants relative to the planning of the phantom test are presented in Table 10. The mean translational error of the isocentre of the implants relative to the planning was  $1.94 \pm 0.79$  mm.

Table 10: Translational error between planned and post-operative implant position on the phantoms.

Subject	Type	Laterality	Cranial glass bead [mm]	Dorsal glass bead [mm]	Caudal glass bead [mm]	Isocentre [mm]
$A_{(p)}$	Phantom	Left	3.12	3.41	3.12	<b>3.17</b>
		Right	3.34	2.03	1.98	<b>2.19</b>
$B_{(p)}$	Phantom	Left	0.97	2.20	3.53	<b>2.03</b>
		Right	0.51	0.80	0.70	<b>0.50</b>
$C_{(p)}$	Phantom	Left	3.10	2.66	3.71	<b>1.63</b>
		Right	2.61	2.73	4.01	<b>2.12</b>
			Mean: 2.28 $\pm 1.12$	Mean: 2.31 $\pm 0.80$	Mean: 2.84 $\pm 1.15$	<b>Mean: 1.94 <math>\pm 0.79</math></b>

The angulation errors of the implants relative to the planning are presented in Table 11. The mean angulation error in the transversal plane was  $2.87 \pm 1.81^\circ$ . In the dorsal plane the mean angular error measured  $1.72 \pm 1.64^\circ$  and in the sagittal plane the error was  $3.10 \pm 2.52^\circ$ .

Table 11: Angulation error between planned and post-operative implant position on the phantoms.

Subject	Type	Laterality	Transversal [°]	Dorsal [°]	Sagittal [°]
A <sub>(p)</sub>	Phantom	Left	3.37	0.23	1.10
		Right	5.24	3.20	1.92
B <sub>(p)</sub>	Phantom	Left	0.66	0.57	3.20
		Right	3.02	0.06	1.53
C <sub>(p)</sub>	Phantom	Left	4.52	1.77	8.55
		Right	0.40	4.50	2.28
			Mean: 2.87 ± 1.81	Mean: 1.72 ± 1.64	Mean: 3.10 ± 2.52

### Cadaveric test

Two personalized acetabular roof implants were placed on the canine cadaver following to the study protocol. The post-operative positions of the implants together with the planned positions of the cadaveric test are shown in Figure 29. Additional views can be found in Appendix B.

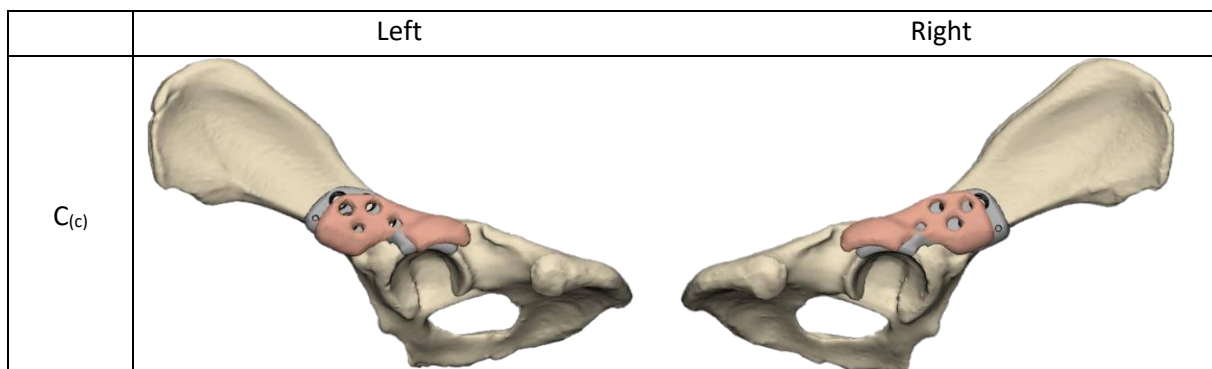


Figure 29: The planned implant positions (gray) and the post-operative implant positions (pink) of the cadaveric test.

The translation errors of the implants relative to the planning in the cadaveric test are presented in Table 12. The mean translational error at the isocentre of the implants was 4.34 mm.

Table 12: Translational error between planned and post-operative implant position on the cadaveric specimen.

Subject	Type	Laterality	Cranial glass bead [mm]	Dorsal glass bead [mm]	Caudal glass bead [mm]	Isocentre [mm]
C <sub>(c)</sub>	Cadaver	Left	6.66	2.85	4.74	<b>3.67</b>
		Right	5.46	4.53	5.54	<b>5.01</b>
			Mean: 6.06	Mean: 3.69	Mean: 5.14	<b>Mean: 4.34</b>

The angulation errors of the implants relative to the planning in the cadaveric test are presented in Table 13. The mean angulation error in the transversal plane was  $3.65^\circ$ . In the dorsal plane the mean angular error measured  $0.41^\circ$  and in the sagittal plane the error was  $4.86^\circ$ .

Table 13: Angulation error between planned and post-operative implant position on the cadaveric specimen.

Subject	Type	Laterality	Transversal [°]	Dorsal [°]	Sagittal [°]
C <sub>(c)</sub>	Cadaver	Left	5.20	0.55	6.09
		Right	2.10	0.26	3.62
			Mean: 3.65	Mean: 0.41	Mean: 4.86

#### In vivo dog patient

The AR/MR-guidance was evaluated during the surgical procedure of implantation of bilateral personalized acetabular roof implants on a dog patient.

On the first side, the patient registration was performed (Figure 30). The user positioned the implant and drilled the screw tunnel using the AR/MR surgical navigation (Figure 31). The veterinary surgeon was however not satisfied about the implant position after reviewing the fluoroscopy images. The veterinary surgeon continued the surgical protocol without AR/MR-guidance.

The patient registration on the second side failed three times. After the fourth attempt, the pelvic hologram was in the correct orientation based on visual inspection. However, the surgical table was moved according to the preferences of the surgical staff. The veterinary surgeon continued the surgical protocol without AR/MR-guidance due to time constraints.



Figure 31: Performing the patient registration in the in vivo dog patient using the registration tool.



Figure 30: Performing the surgical navigation in the in vivo dog patient using the navigation tool.

## 4.4 Discussion

### Summary

Six implants have been implanted on canine pelvic phantoms and two on a cadaveric pelvis using HoloMA's AR/MR surgical guidance. No implants were placed in the in vivo dog patient.

The implants on the phantoms demonstrated a maximum translational error of 3.17 mm at the isocentre (mean:  $1.94 \pm 0.79$  mm) and a maximum angulation error of  $8.55^\circ$  relative to the planned position. Two of the six implants did not fulfil the goal of  $<4.0$  mm and/or  $<5.0^\circ$  ( $A_{(p)}$  right and  $C_{(p)}$  left). The left implant on the cadaver fulfilled the goal of the translation error, but not the goal of the angulation error. On the right side of the cadaver this was vice versa.

### Limitations and recommendations

The most likely explanation of the differences between the phantoms and the cadaver is the fact that the patient registration result can be checked more easily on the phantoms since the user has vision on the full bone. The user repeated the patient registration process when the contours of the holographic bone did not match with the phantom. On the cadaver and in the in vivo dog patient only a small portion of the bone can be seen due to the surrounding soft tissue. This made it difficult to judge if the patient registration was performed accurately. For future tests using AR/MR guidance on phantoms, it is recommended to simulate the intra-operative surgical situation by covering the bone in areas that are normally not visible. (20)

Furthermore, contrary to the findings of the in silico patient registration test (chapter 2), it should be noted that the patient registration in all phases was challenging in terms of success. In multiple occasions the holographic iliac bone was positioned upside down based on the obtained point cloud. This issue can potentially be solved by performing an additional point-to-point registration process for the initial alignment of the hologram.

Although the cadaver and in vivo dog patient were carefully fixated to the surgical table, a major methodological limitation in this pilot study is that no reference fiducial was used to compensate for motion. During both the cadaveric and in vivo dog patient test, a reference fiducial was placed initially, but later removed because it could not be detected (cadaveric test) or was hindering the surgical procedure (in vivo test). Motion might have been the cause for the differences between the implants placed on the phantoms and on the cadaver. It is highly recommended to find a solution to place the reference fiducial on the iliac bone in a way that it is within the field of view of the HoloLens 2 camera but not hindering the surgical procedure.

It also should be noted that the locking screw thread of the implants used in the phantom test was vulnerable because they were 3D printed from resin. The locking screws that were used to fixate the implant could easily damage the screw thread to nullify the locking feature. This could have led to a biased orientation of the implant compared to the situation in which the locking tread is still in tact. It is therefore recommended to perform additional analysis to the position of the implanted screws relative to the pre-operatively planned position.

In this pilot study, only a small number of implants were placed using the HoloMA AR/MR-guidance. More implants should be placed in order to validate this new technology. The results of the AR/MR-guided implant positions should also be compared to the personalized acetabular roof implants that were positioned without AR/MR-guidance. Currently there is no access to this confidential data for comparison. Studies that have used a similar AR/MR point cloud patient registration technique report a comparable translational and angulation errors in phantom tests (20-22) and in cadaver tests. (23-26)

## 5 General discussion

### Summary

AR/MR-guidance of HoloMA was introduced and tested in orthopaedic surgery for navigation of personalized acetabular roof implants. A universal tool was designed to perform the patient registration. For the surgical navigation, tools were designed to mount a tracking fiducial to a personalized acetabular roof implant via drill guides. The in silico patient registration test revealed a mean translational error of  $0.94 \pm 0.23$  mm and a mean angulation error of  $2.49 \pm 0.34^\circ$ . Pilot tests were conducted to determine the accuracy of the implant position on phantoms, cadavers and an in vivo dog patient. Four out of eight of these AR/MR-guided implants were positioned with a translational error less than 4.0 mm and an angulation error less than  $5.0^\circ$ .

### Recommendations for future work

More phantom tests should be conducted before further employment of HoloMA AR/MR surgical guidance for personalized acetabular roof implants. The results of these phantom tests should show at least similar results in terms of translational and angulation error compared to the implants that are placed in dog patients without AR/MR guidance. The AR/MR-guided implant positions should also be analysed in terms of clinical success regarding the amount of coverage of the femoral head. (27) If these results are similar (or better) than the freehand positioned implants in dog patients, the AR/MR-guidance has the potential to be beneficial in more challenging situations such as in cadavers.

When conducting additional tests on cadavers and/or in vivo dog patients, it is advisable to start with a study protocol in which only the AR/MR patient registration is performed. The hologram of the implant superimposed on the real iliac bone will then only serve as a suggestion where to position the implant. This will not determine the accuracy of the AR/MR software as the user has the freedom to deviate from the suggested position, but only having this suggested position as a hologram might already be beneficial in terms of implant placement compared to the non-AR/MR guided procedure.

The major issue that was encountered during this project was the detectability rate of the fiducial markers. The HoloMA software often could not detect these fiducials causing to interrupt the patient registration and/or the surgical navigation temporarily. The fiducial markers used in this project were laser engraved from plastic. It could be that the light was reflected too much from the plastic surface into the RGB camera of the HoloLens 2 under specific angles. The underlying cause could also be a limitation of the HoloLens 2 RGB-camera itself or a limitation of the HoloMA software. Alternative (sterilizable) materials for the fiducials should be considered to minimize the reflection. It should also be considered to use cubic fiducials with unique black-and-white patterns on each face instead of the planar fiducials. If one face is subjected to reflection, it might be possible to still detect one or more adjacent faces. (28) Besides, a marker with multiple faces might increase depth perception. (29)

It is highly recommended to invest in the ability to share the view of the AR/MR holograms to the other members of the surgical team (e.g. other surgeons and surgical assistants). The most ideal way is to do this by coupling multiple AR/MR displays so the others can join the virtual world and see and interact with the holograms in 3D. During this project, the multiplayer feature of HoloMA was still under development. As an alternative, the live video from the HoloLens 2 camera including the holograms was streamed to a 2D monitor. This allowed discussion with the other team members, but the user of the AR/MR display remained the only person to be able to interact with the virtual world.

In addition to the multiplayer feature, it is also advised to develop an application that can be run on an external device (e.g. smartphone or computer tablet) which allows a non-sterile member of the team to interact with the AR/MR software. The sterile person(s) with the AR/MR display(s) can then keep focus on the surgical field while the settings of the AR/MR software are managed via the external device.

## 6 Conclusion

The results of the in silico patient registration test are promising for the AR/MR-guidance of personalized acetabular roof implants. Placing these implants on phantoms using the AR/MR-guidance however showed moderate results. Using the AR/MR surgical navigation for placement of the personalized acetabular roof implants on cadavers and in vivo cases is currently not advised.

## 7 References

- (1) Yang S, Zusman N, Lieberman E, Goldstein RY. Developmental Dysplasia of the Hip. *Pediatrics* 2019;143(1):e20181147.
- (2) Cooperman D. What is the evidence to support acetabular dysplasia as a cause of osteoarthritis? *J Pediatr Orthop* 2013 August 01;33 Suppl 1:2.
- (3) Clohisy JC, Schutz AL, St John L, Schoenecker PL, Wright RW. Periacetabular osteotomy: a systematic literature review. *Clin Orthop Relat Res* 2009 August 01;467(8):2041-2052.
- (4) Clohisy JC, Nunley RM, Curry MC, Schoenecker PL. Periacetabular osteotomy for the treatment of acetabular dysplasia associated with major aspherical femoral head deformities. *J Bone Joint Surg Am* 2007 July 01;89(7):1417-1423.
- (5) Gillingham BL, Sanchez AA, Wenger DR. Pelvic osteotomies for the treatment of hip dysplasia in children and young adults. *J Am Acad Orthop Surg* 1999 October 01;7(5):325-337.
- (6) Bartonicek J, Vavra J, Chochola A. Bosworth hip shelf arthroplasty in adult dysplastic hips: ten to twenty three year results. *Int Orthop* 2012 December 01;36(12):2425-2431.
- (7) König F. Osteoplastische behandlung der kongenitalen hueftgelenluxation (mit demonstration eines pareparates). *Verh Dtsch Ges Chir* 1891;20:75-80.
- (8) Staheli LT, Chew DE. Slotted Acetabular Augmentation in Childhood and Adolescence. *Journal of Pediatric Orthopaedics* 1992;12(5).
- (9) Fawzy E, Mandellos G, De Steiger R, McLardy-Smith P, Benson MK, Murray D. Is there a place for shelf acetabuloplasty in the management of adult acetabular dysplasia? A survivorship study. *J Bone Joint Surg Br* 2005 September 01;87(9):1197-1202.
- (10) Shibata KR, Matsuda S, Safran MR. Open treatment of dysplasia-other than PAO: does it have to be a PAO? *J Hip Preserv Surg* 2015 May 13;4(2):131-144.
- (11) Kirkby KA, Lewis DD. Canine hip dysplasia: reviewing the evidence for nonsurgical management. *Vet Surg* 2012 January 01;41(1):2-9.
- (12) Willemsen K, Tryfonidou MA, Sakkera RJB, Castelein RM, Beukers M, Seevinck PR, et al. Patient-specific 3D-printed shelf implant for the treatment of hip dysplasia tested in an experimental animal pilot in canines. *Scientific Reports* 2022;12(1):3032.
- (13) Loeser RF. The Role of Aging in the Development of Osteoarthritis. *Trans Am Clin Climatol Assoc* 2017;128:44-54.
- (14) McCloskey K, Turlip R, Ahmad HS, Ghenbot YG, Chauhan D, Yoon JW. Virtual and Augmented Reality in Spine Surgery: A Systematic Review. *World Neurosurg* 2023 May 01;173:96-107.
- (15) Birlo M, Edwards PJE, Clarkson M, Stoyanov D. Utility of optical see-through head mounted displays in augmented reality-assisted surgery: A systematic review. *Med Image Anal* 2022 April 01;77:102361.
- (16) Ma L, Huang T, Wang J, Liao H. Visualization, registration and tracking techniques for augmented reality guided surgery: a review. *Phys Med Biol* 2023 February 17;68(4):10.1088/1361-6560/acaf23.
- (17) Doughty M, Ghugre NR, Wright GA. Augmenting Performance: A Systematic Review of Optical See-Through Head-Mounted Displays in Surgery. *J Imaging* 2022 July 20;8(7):203. doi: 10.3390/jimaging8070203.

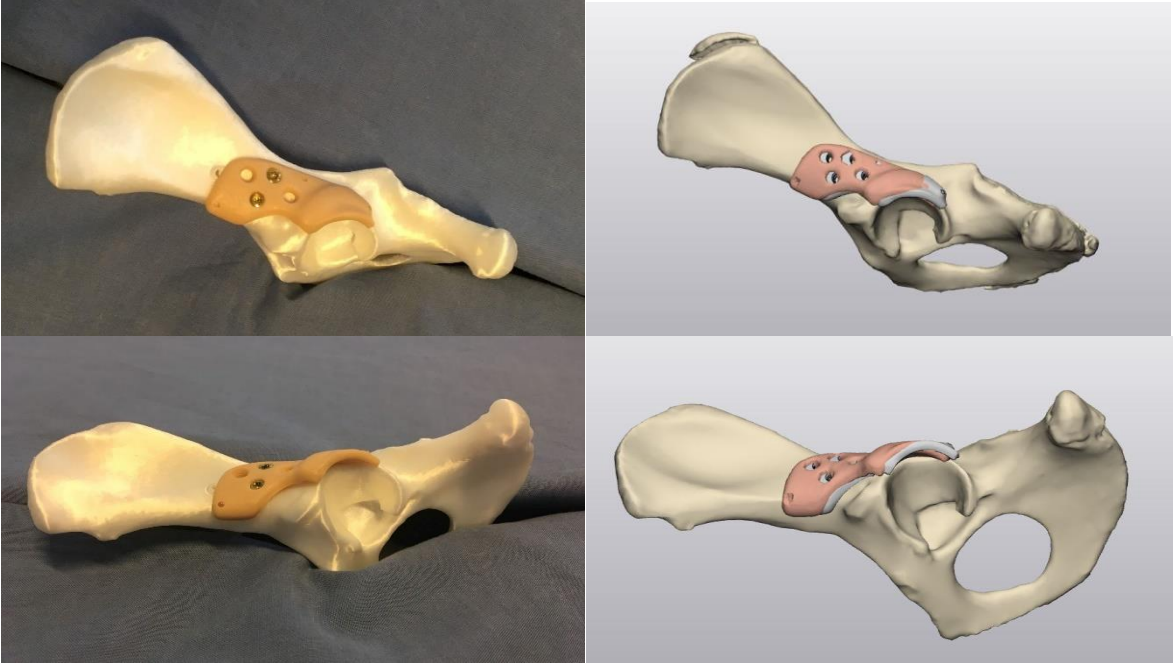
- (18) Kwananocha I, Magre J, Willemsen K, Weinans H, Sakkers RJB, How T, et al. Acetabular rim extension using a personalized titanium implant for treatment of hip dysplasia in dogs: short-term results. *Front Vet Sci* 2023 April 20;10:1160177.
- (19) Stoutjesdijk SR. Patient registration strategies without intra-operative radiological imaging in Extended Reality guided skeletal surgery: a review. (unpublished) 2023.
- (20) Kiarostami P, Dennler C, Roner S, Sutter R, Furnstahl P, Farshad M, et al. Augmented reality-guided periacetabular osteotomy-proof of concept. *J Orthop Surg Res* 2020 November 17;15(1):540-x.
- (21) Liebmann F, Roner S, von Atzigen M, Scaramuzza D, Sutter R, Snedeker J, et al. Pedicle screw navigation using surface digitization on the Microsoft HoloLens. *Int J Comput Assist Radiol Surg* 2019 July 01;14(7):1157-1165.
- (22) Kriechling P, Roner S, Liebmann F, Casari F, Furnstahl P, Wieser K. Augmented reality for base plate component placement in reverse total shoulder arthroplasty: a feasibility study. *Arch Orthop Trauma Surg* 2021 September 01;141(9):1447-1453.
- (23) Spirig JM, Roner S, Liebmann F, Furnstahl P, Farshad M. Augmented reality-navigated pedicle screw placement: a cadaveric pilot study. *Eur Spine J* 2021 December 01;30(12):3731-3737.
- (24) Farshad M, Spirig JM, Suter D, Hoch A, Burkhard MD, Liebmann F, et al. Operator independent reliability of direct augmented reality navigated pedicle screw placement and rod bending. *North American Spine Society Journal (NASSJ)* 2021;8:100084.
- (25) Kriechling P, Loucas R, Loucas M, Casari F, Furnstahl P, Wieser K. Augmented reality through head-mounted display for navigation of baseplate component placement in reverse total shoulder arthroplasty: a cadaveric study. *Arch Orthop Trauma Surg* 2021 July 02.
- (26) Ackermann J, Liebmann F, Hoch A, Snedeker JG, Farshad M, Rahm S, et al. Augmented Reality Based Surgical Navigation of Complex Pelvic Osteotomies—A Feasibility Study on Cadavers. *Applied Sciences* 2021;11(3).
- (27) Willemsen K, Tryfonidou M, Sakkers R, Castelein RM, Zadpoor AA, Seevinck P, et al. Patient-specific 3D-printed shelf implant for the treatment of hip dysplasia: Anatomical and biomechanical outcomes in a canine model. *J Orthop Res* 2022 May 01;40(5):1154-1162.
- (28) Simões RJ, Raposo C, Barreto J, Edwards PJ, Stoyanov D. Visual Tracking vs Optical Tracking in Computer-Assisted Intervention. 2018.
- (29) Tu P, Gao Y, Lungu AJ, Li D, Wang H, Chen X. Augmented reality based navigation for distal interlocking of intramedullary nails utilizing Microsoft HoloLens 2. *Comput Biol Med* 2021 June 01;133:104402.

8 Appendixes

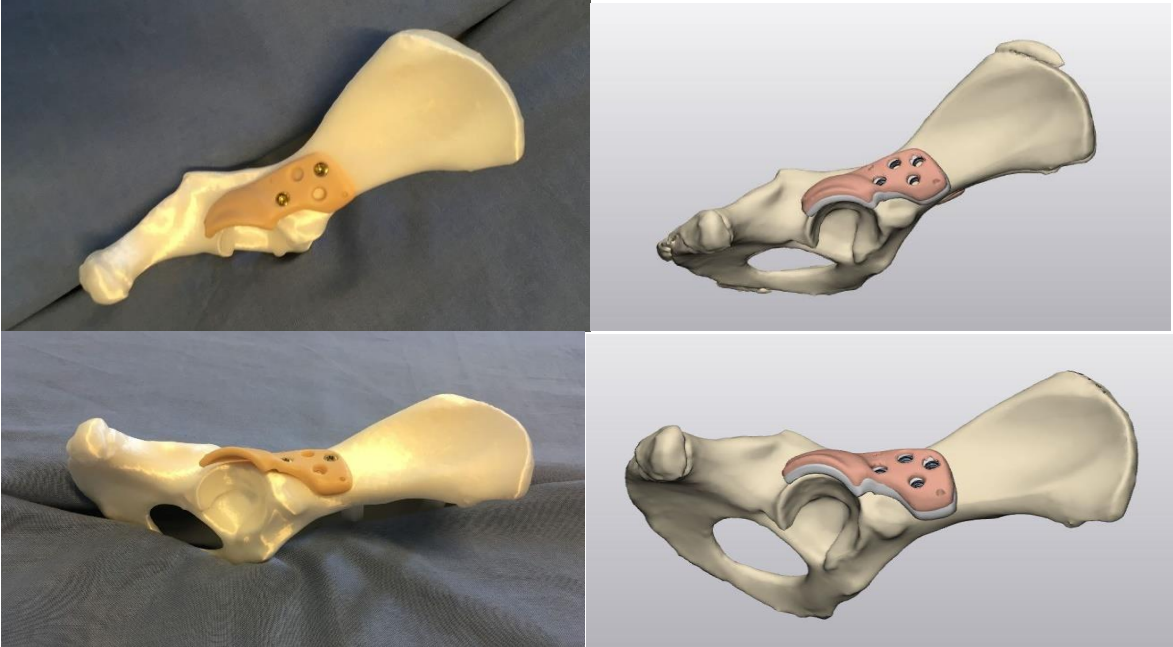
Appendix A: Implant position on phantoms

Subject A<sub>(p)</sub>

Left

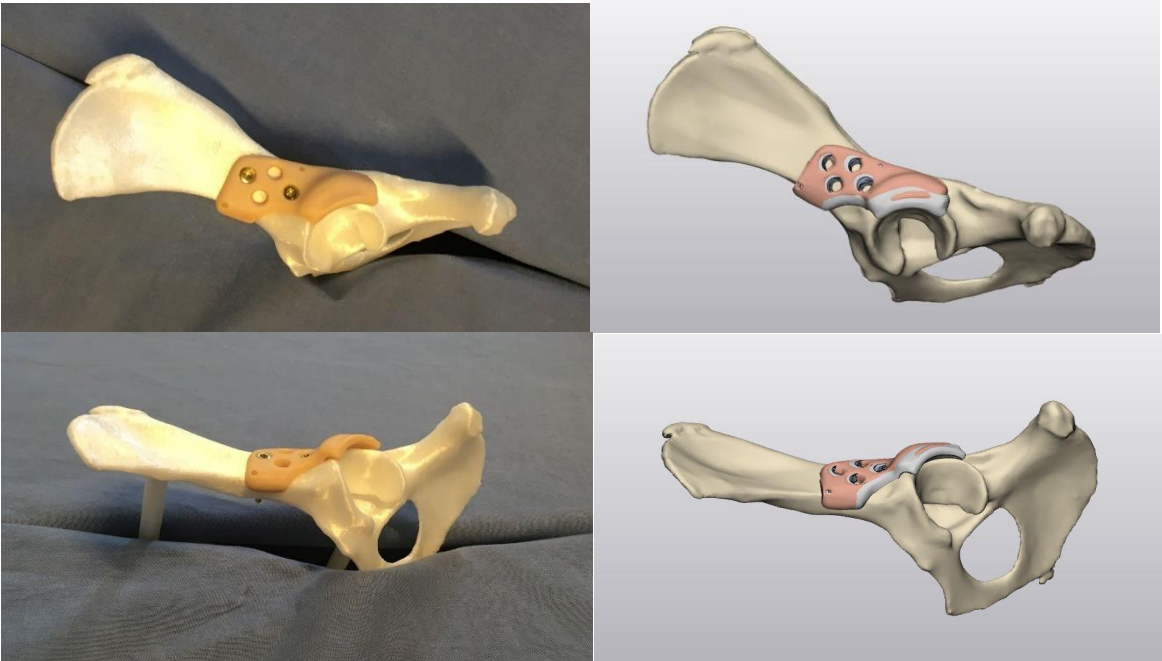


Right

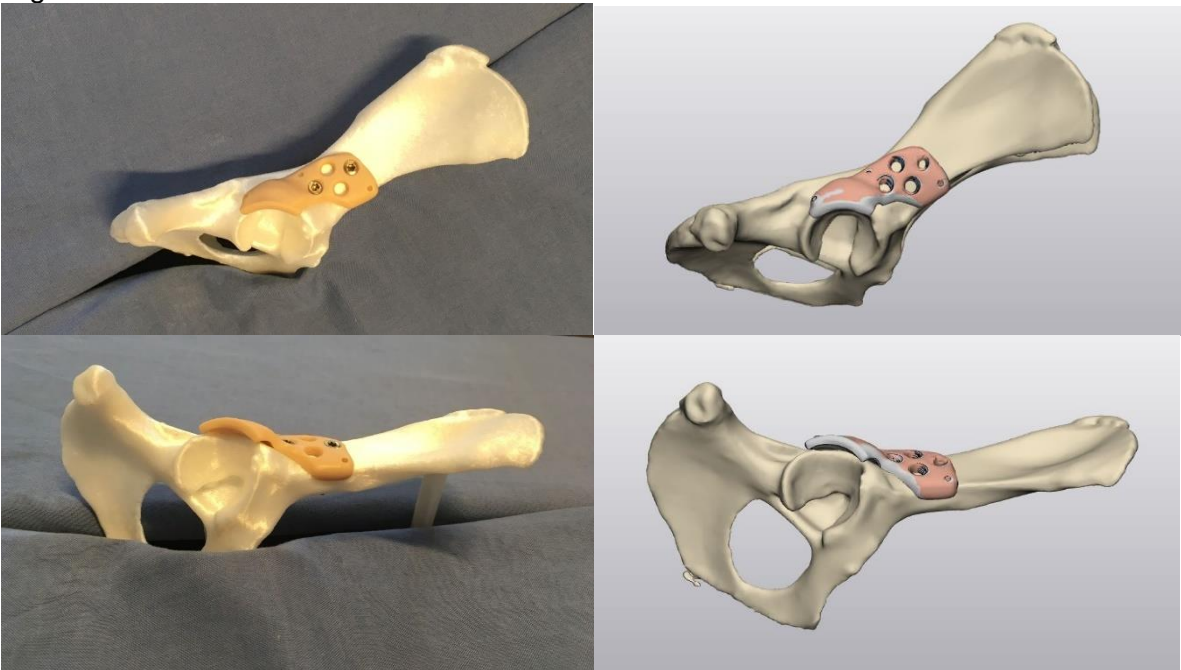


Subject B<sub>(p)</sub>

Left

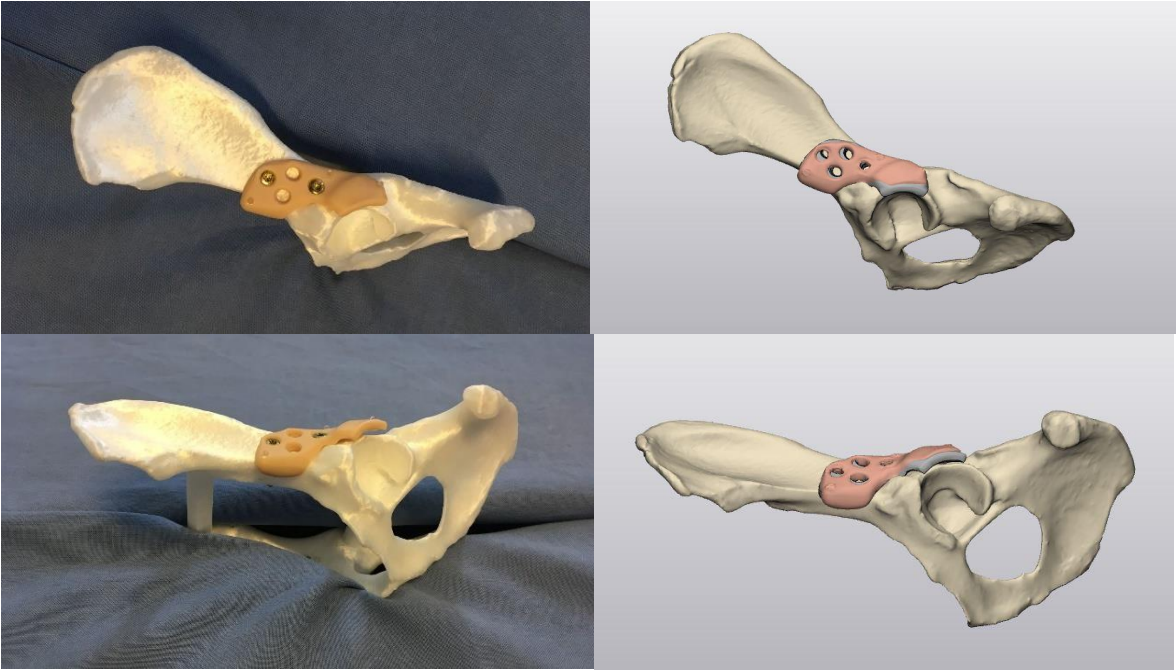


Right

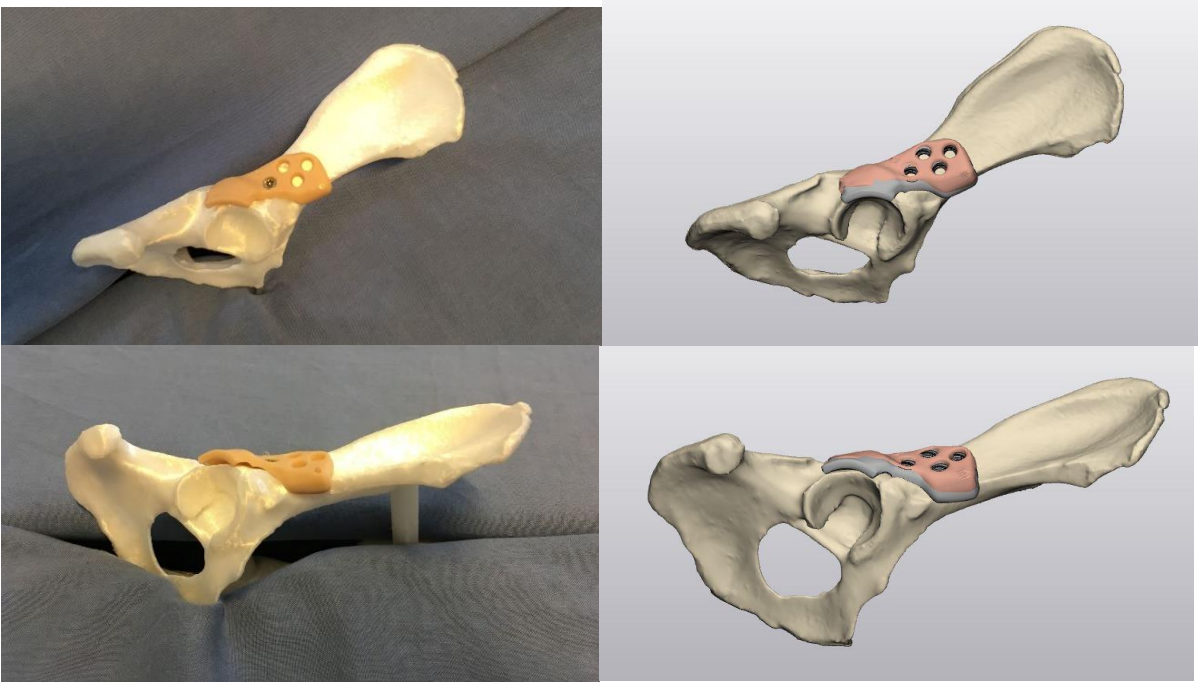


Subject C<sub>(p)</sub>

Left



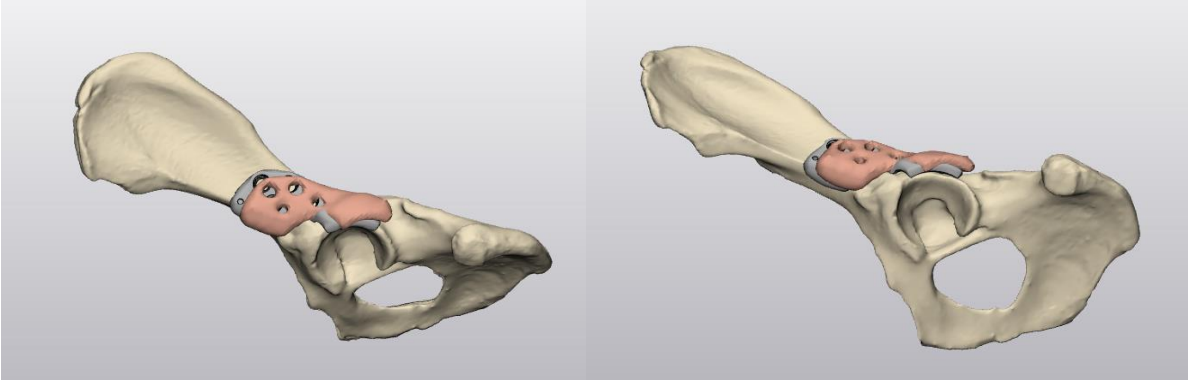
Right



Appendix B: Implant position on cadaver

Subject C<sub>(c)</sub>

Left



Right

